2013

Computer Code Verification and Cross Section Calculation for Promethium-147

Rita Inez Zell-Lusk
rzell@vols.utk.edu

Computer Code Verification and Cross Section Calculation for Promethium-147

A Practice Project
Presented for the
Master of Science Degree
The University of Tennessee, Knoxville

Rita Inez Zell Lusk

November 2013

ACKNOWLEDGEMENTS AND DEDICATION

I would like to thank Dr. Lawrence Heilbronn for serving as my faculty advisor and Dr. Ivan Maldonado and Dr. Howard Hall for serving on my masters committee. I would also like to thank Dr. Saed Mirzadeh of Oak Ridge National Lab for his guidance. Thank you to David Denton, Greg Hirtz, George Askew, and Jeff Pryor for helping to prepare and certify NM-784 for irradiation. Previous researchers on this project include James Hinderer, Kathleen Broderick, and Rose Boll. This Research was supported by the DOE, Office of Nuclear Physics, Isotope program, under contract DE-AC05-00OR22725 with UT-Battelle, LLC.

I would like to thank members of Dr. Heilbronn's ORNL-based research group, Chelsea Burnham, Justin Griswold, and Spenser Walsh. I would also like to thank those who have helped me along the way, including Price Collins for aiding in the solving of one particularly nasty equation.

On a personal note, all glory goes to God and it is through science that I see Him clearly. My family has been of tremendous support. To my Dad, Paul Zell, thank you for instilling in me a love for science and of course, bad science jokes. To my Mom, Elizabeth, for showing me by example what hard work and perseverance (even in the face of certain failure) is all about. To my husband, Greg, thank you for standing by my side through this graduate school adventure. Of course, this section would not be complete without mentioning my writing buddy, Baxter the orange tabby cat.

TABLE OF CONTENTS

1. Introduction, Purpose, and Scope

1.1 Description of and Uses for Pm-147

Promethium-147 has a half-life of 2.62 years and is a soft beta emitter with endpoint energy of 224.5 keV and an average energy of 62 keV. It also has a weak gamma ray at 121.2 keV with intensity of 2.85E-3%. Promethium is a rare-earth element in the Lanthanide Series with an atomic number of 61, as seen below in Figure 1.1.

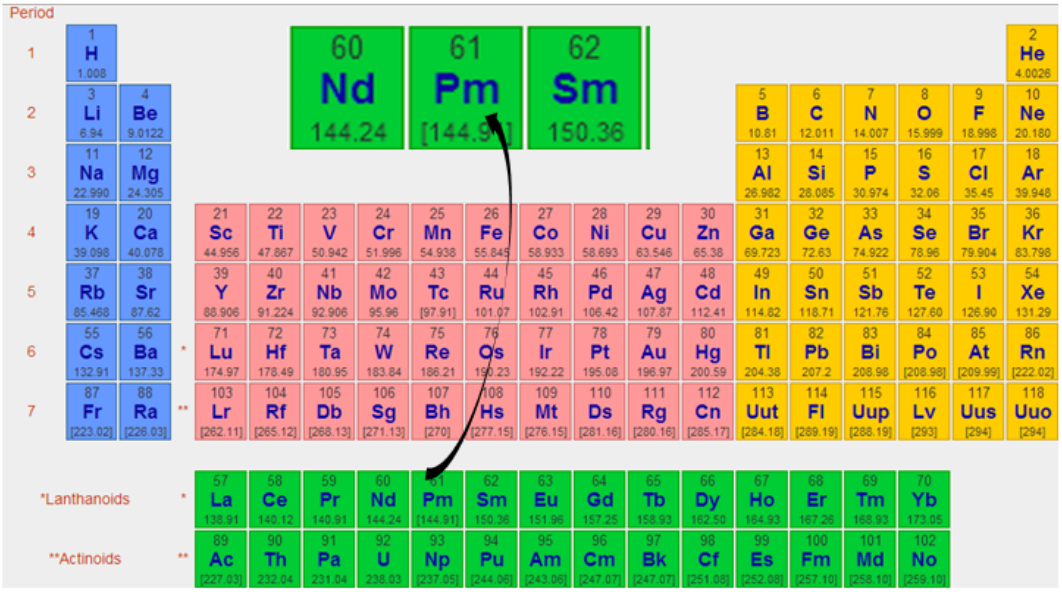

Figure 1.1: Table of the Elements Showing Neodymium, Promethium, and Samarium (Figure courtesy of www.webelements.com [19])

Promethium does not exist in nature and all of its isotopes are radioactive. Traditionally, Pm-147 was acquired from the processing of spent nuclear reactor fuel. Since there is no more U.S. spent nuclear fuel processing and all the stores of Pm-147 have been exhausted, an alternate method of production, such as the neutron capture method, must be used. A highly enriched target of stable Nd-146 is irradiated with neutrons and the result from a single neutron capture, Nd-147, decays by beta emission with a half-life of 10.98 days to produce Pm-147. Assay of Pm-147 is difficult because its 121.2 keV gamma ray is not immediately visible after production because of the higher intensity 120.5 keV gamma ray from Nd-147. This is illustrated below in Figure 1.2.

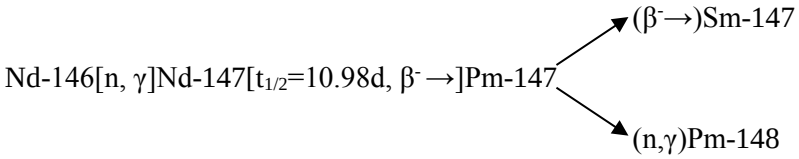

Figure 1.2: Single Neutron Capture and Decay

Nd-147 has a maximum beta energy of 896.1 keV and decays to Pm-147 100% of the time, and Pm-147 has a maximum beta energy of 224.1keV and decays to Sm-147 99.994% of the time, as seen below in Figures 1.3-4.

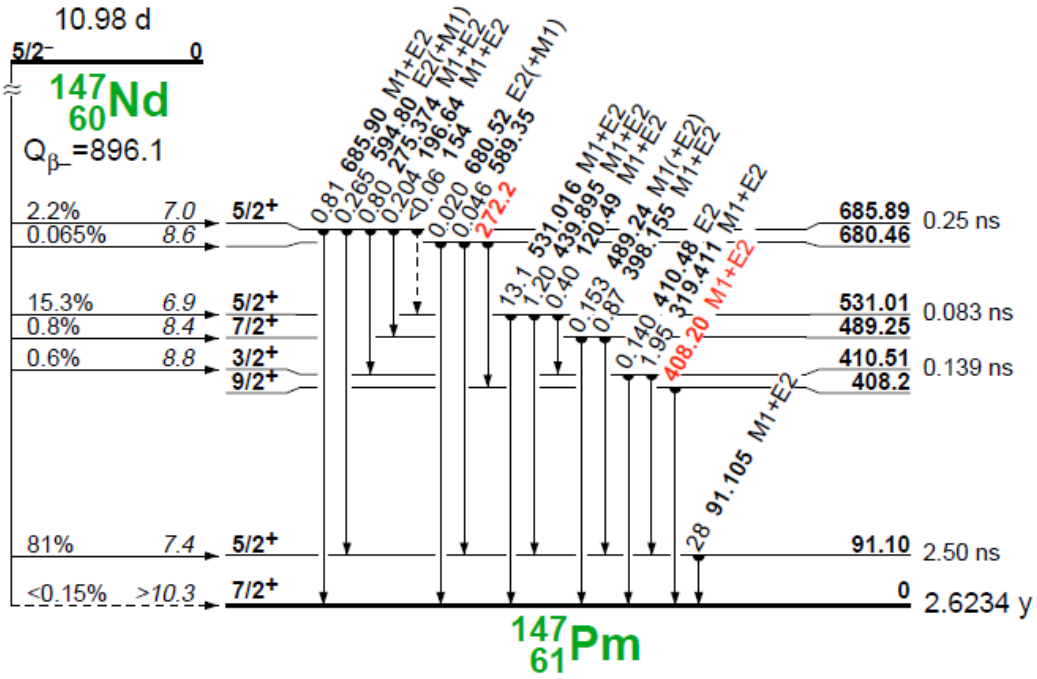

Figure 1.3: Decay Scheme of Nd-147 (Figure Courtesy of Table of Isotopes by Firestone and Shirley [15])

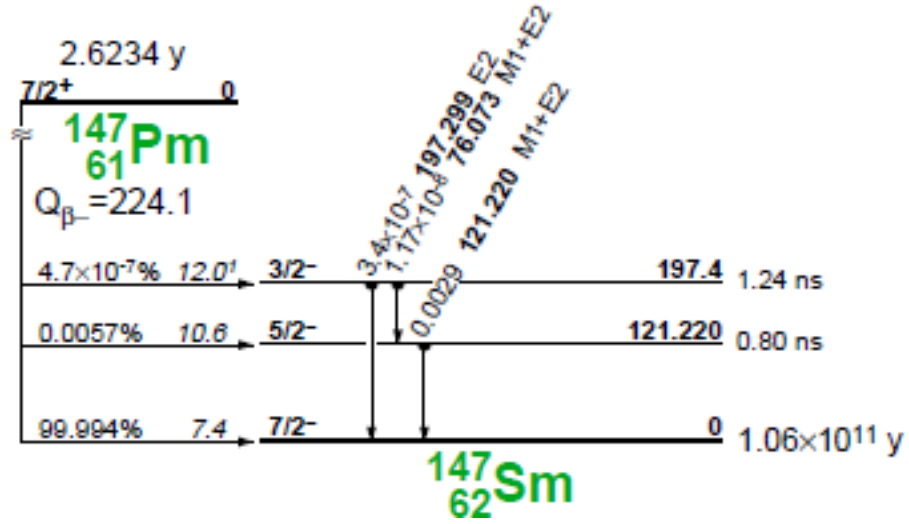

Figure 1.4: Decay Scheme of Pm-147 (Figure Courtesy of Table of Isotopes by Firestone and Shirley [15])

Pm-147 is a desired isotope because of its use as a nuclear battery. A nuclear battery is a device that uses a nuclear reaction instead of a chemical reaction to produce an electrical current. Nuclear batteries are hailed as the battery of the future because of their long life and improved reliability. For instance, a battery powered by Pm-147 can power a device for about 5 years. Current uses of nuclear batteries include space applications, where their long life is a necessity on long missions. In addition, they produce heat that is used to heat electronics on spacecraft in the cold vacuum of space. They also can be employed in medical devices such as pacemakers and implanted defibrillators. Nuclear batteries can also be used to power mobile devices for civilian and military use. The military is interested in nuclear batteries because they are lighter, longer lasting, and more reliable than conventional batteries. Military applications include sensors, ultra-wide-band communication chips, and "smart dust" sensors. Nuclear batteries can also be used on probes and sensors deployed under the ocean. However, drawbacks include high initial cost, laws governing disposal and use of radioactive materials, and the general public's aversion to radiation. [6]

There are many candidate radioactive isotopes, but only about 100 of them have half-lives of acceptable length for use in nuclear batteries (100 days to 100 years). Limiting the criteria even further, to requiring the specific power to be greater than 0.1 Watt(thermal)/gram narrows the list to 30. A few of these favorable isotopes are listed below in Table 1.1.

Table 1.1: A Few Isotopes of Interest for Power Generation [7]

Isotope	Types of Radiation Emissions	Half-life	Specific Power (Watts (th)/gram)
Tritium	β-, no γ	12.33 y	0.26
Cobalt-60	β-, γ	5.27 y	17.7
Strontium-90	β-, no γ	29 y	0.93
Promethium-147	β-, few γ	2.62 y	0.33
Polonium-210	α, few γ	136.38 d	141
Plutonium-238	α, γ, SF	87.74 y	0.56

Promethium-147 is advantageous because it has one of the higher specific activities among the beta emitters. While Strontium-90 has a higher specific activity than Pm-147, its half life is too long for some applications. Cobalt-60 also has a higher specific activity than Pm-147, but it has more intense gamma rays that can make it more difficult to use for some applications due to increased shielding requirements. These properties make Pm-147 an ideal isotope for some applications of nuclear batteries, and worth researching and developing.

1.2 Purpose

The goals of this research are to (1) verify the predictions and accuracy of two computer codes which will be utilized in future research on Pm-147 production with data from a previous experiment and to (2) measure the cross section of Pm-147 for single neutron capture producing Pm-148 ground state and Pm-148 metastable state.

1.3 Scope

The research outlined in goal (1) above used previous data obtained by James H. Hinderer in 2010 and a sample of Promethium-147 prepared by Rose Boll in 2006. The research utilized Oak Ridge National Laboratory's High Flux Isotope Reactor (ORNL HFIR). The main elements of the new research done here included a correction of Mr. Hinderer's data and then the use of the corrected data to verify the Cumming's Least Square Method ('CLSQ') and the Isochain computer codes. To achieve the results outlined in goal (2) above, new HFIR irradiations were performed to measure the cross-section of Promethium-147 for single neutron capture was also measured, irradiating a previously prepared sample of Pm-147 in HFIR to make Pm-148 ground and Pm-148 metastable states.

2. Detector Efficiency

The first part of the research done on Promethium-147 was done using a detector located in Building 4501 Room 127a on the ORNL campus. The detector is a Canberra High Purity Germanium detector. The detector efficiency needed to be calculated and applied to the raw data before the data could be used for code verification. A multi-gamma standard was counted on each shelf and the program Efficurve was used to analyze the calibration data. It is a program that takes data from a detector obtained from using a standard with multiple gamma rays. It then calculates an equation that can be used to calculate efficiencies for any shelf at any energy that is needed. To begin, data from measuring the multi-gamma standard were tabulated and then the efficiency and error for each peak on the multi-gamma standard was calculated to form an input document for Efficurve. The following set of equations were used:

$$col(4)=e^{(-(col(3)*t_{decay}))} \quad [2.1]$$

$$col(5)=col(2)*col(4) \quad [2.2]$$

$$col(7)=col(6)/col(5) \quad [2.3]$$

$$col(10)=col(9)/col(6) \quad [2.4]$$

$$col(11)=col(10)*col(7) \quad [2.5]$$

Where:

e=2.7182818282846

t_{decay} = Decay Time for the source used

col(2) = Initial Emission rate for each energy (from the multigamma standard's documentation sheet)

col(3) = Decay Constant of isotope in question

col(5) = Calculated activity at time of count

col(6) = counts per second at the energy in question from detector output

col(7) = Efficiency

col(9) = Error at the energy in question from detector output

col(10) = Relative Error

The Efficurve program inputs are the energy, efficiency (col(7) above), and error (col(11) above). Also, the operator inputs to the program how many constants it should produce. The program then outputs a functional form and the number of constants that the operator told it to produce. The form of the function produced is:

$$\text{Effciency} = \exp[C1+C2*\ln(x)+C3*(\ln(x))^2+C4*(\ln(x))^3+C5*(\ln(x))^4] \qquad [2.6]$$

Where C1, C2, C3, C4, and C5 are constants produced by Efficurve. The constants that Efficurve produced for shelf 20 of the detector in ORNL's building 4501, room 127a are listed below in Table 2.1:

Table 2.1: Constants for Efficiency Calculations for Shelf 20 as Example

Constant	Efficiency
1	-1.53E+02
2	1.05E+02
3	-2.75E+01
4	3.14E+00
5	-1.34E-01

The efficiencies for all of the detector shelves measured in graph form are shown below in Figure 2.1:

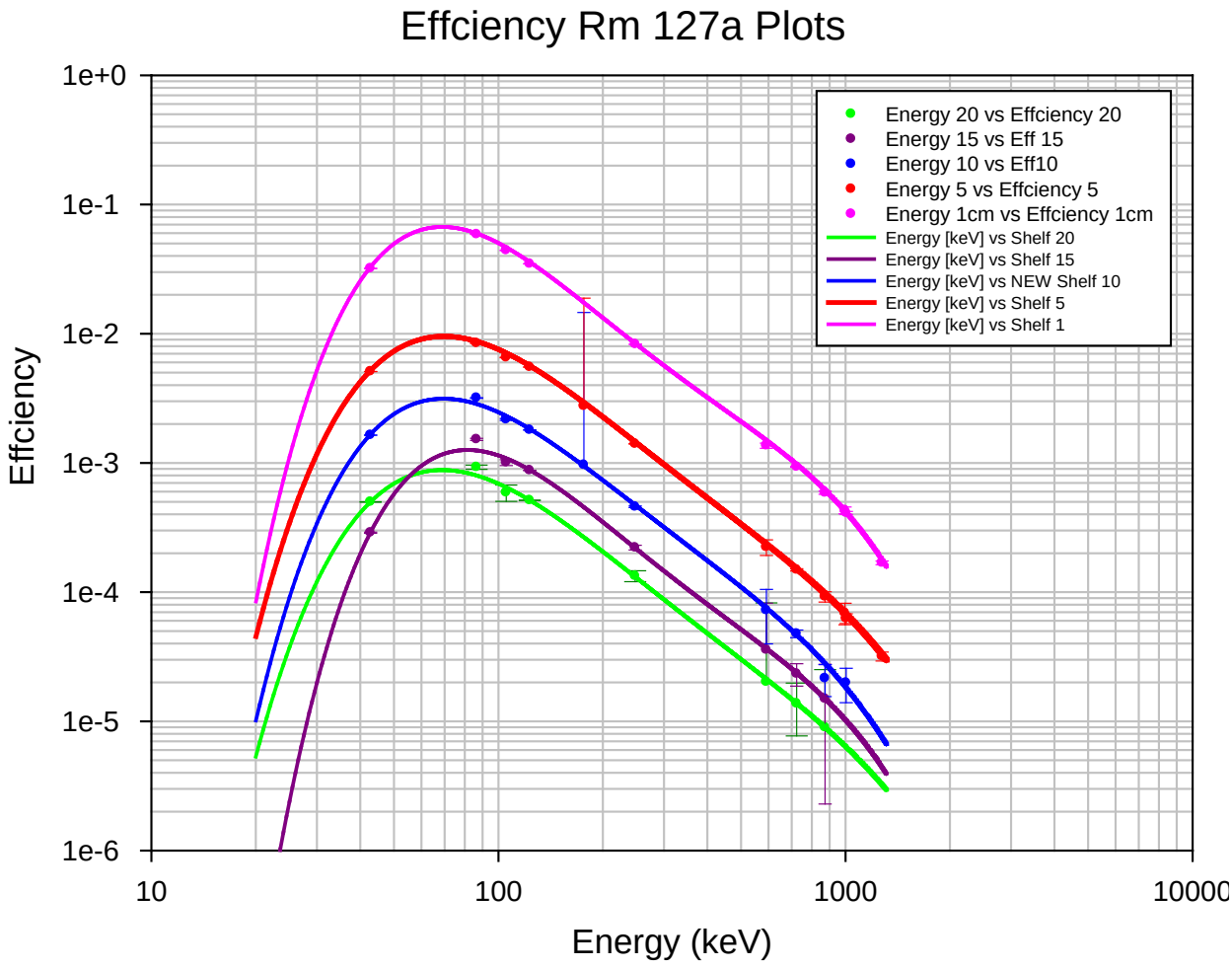

Figure 2.1: Efficiencies of ORNL Room 127a Detector for each shelf

The efficiencies are tabulated below in Table 2.2 for the shelves of interest at 121.26 keV:

Table 2.2: Efficiencies of Interest for Experiment:

Room/Shelf	Efficiency
127A/20	0.000526542
127A/15	0.000895181
127A/10	0.001844353
127A/5	0.005643542
127A/1	0.035661100
126/1	0.07412281

3. *Previous Data Analysis and Correction*

This project continues the work that James Hinderer did for his Master of Science thesis in May 2010 entitled "Radioisotopic Impurities in Promethium-147 Produced at the ORNL High Flux Isotope Reactor (HFIR)". [21] He prepared a sample of Neodymium-146 (given the number 'NM-668') for irradiation in Oak Ridge National Laboratory's High Flux Isotope Reactor. Neodymium-147 was produced by neutron bombardment of Nd-146, which decayed to Promethium-147. This is referred to as the neutron capture route.

$$^{146}\mathrm{Nd}[n,\gamma]\ ^{147}\mathrm{Nd}(t_{1/2}=10.98\mathrm{d},\ \beta^-) \longrightarrow\ ^{147}\mathrm{Pm} \qquad [3.1]$$

After the sample cooled enough to be handled, 10% of the sample was removed from the target and counted in High Purity Germanium detectors located in ORNL's Building 4501 Room 126 and 127A. Counting began at 46 days post bombardment. As the Nd-147 decayed with a half-life of 10.98 days, the Pm-147 with a half-life of 2.62 years grew in. This change is visible at approximately 150 days post bombardment, as shown in the logarithmic plots shown below. Figure 3.1 shows the raw data graphed as counts per minute versus decay time in days post bombardment. The error is so low that it is hard to see the error bars through the plotted points.

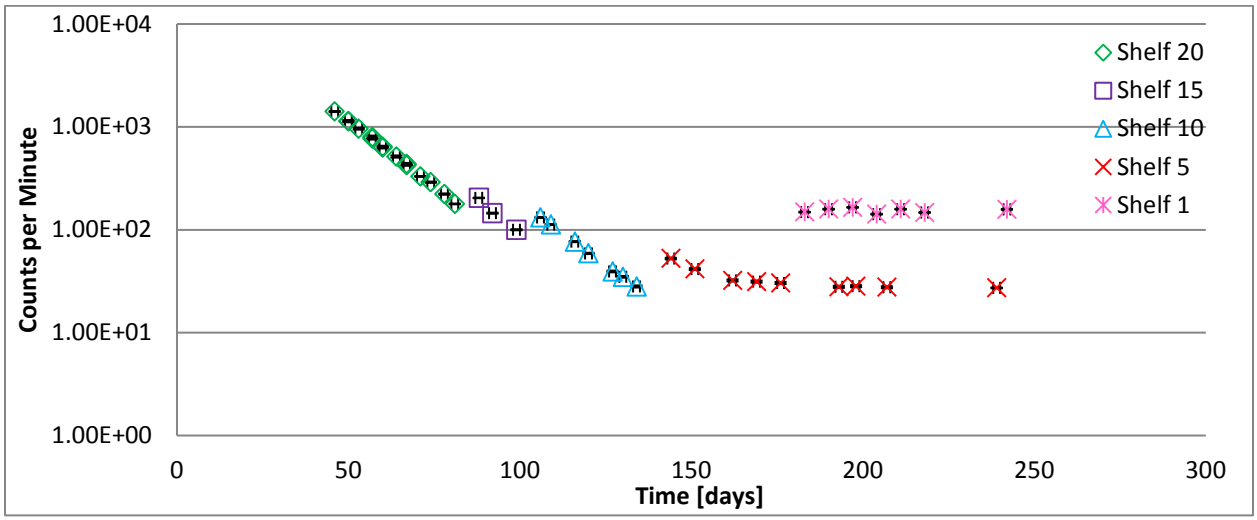

Figure 3.1: Neodymium-147 and Promethium-147 Decay Without Correction

As is shown in the above figure, the plotted data is not continuous, as would have been expected from radioactive decay. The reason for this is that the sample NM-668 was moved to shelves closer and closer to the detector as the number of days post bombardment so that the sample would not have to be counted as long to get enough counts to analyze. It was thought that dividing the data by a certain factor, related to the detector shelf efficiency would solve this problem and make the data continuous. This is referred to as the "Geometrical Correction Factor" or "GCF". First, a shelf was picked to be the 'standard' shelf. Shelf 20, the shelf that the counting started on, was selected as the standard shelf. The Geometrical Correction Factor is the ratio of the efficiency of the shelf of interest to the efficiency of the standard shelf. Table 3.1

below shows the Geometrical Correction Factor for the detector shelves used in this experiment. For example:

$$GCF = \frac{Effciency(Shelf\,15)}{Effciency(Shelf\,20)} = \frac{0.000895180}{0.000526542} = 1.7001 \qquad [3.2]$$

Table 3.1: Geometrical Correction Factors for Shelves Used in Experiments:

Room/Shelf	GCF
127A/20	1
127A/15	1.7001
127A/10	3.5028
127A/5	10.7181
127A/1	67.7269
126/1	140.7728

When these factors are divided by the data that is plotted in Figure 3.1 above, a continuous line for radioactive decay is shown below in Figure 3.2. The error is so low that it is hard to see the error bars through the plotted points.

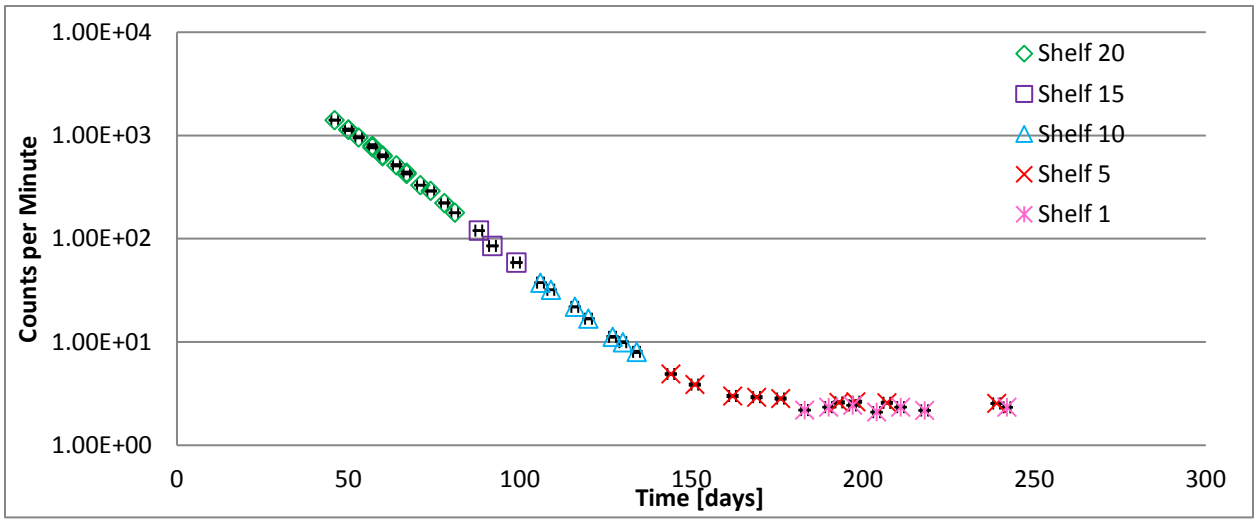

Figure 3.2: Neodymium-147 and Promethium-147 decay with Geometrical Correction Factor

4. Computer Code Validation

4.1 CLSQ

CLSQ, or Cumming's Least Square method, is a computer program that fits a least square curve to the inputted data taken from nuclear decay measurements. It was specifically made to use the least squares method to fit a curve to data from nuclear decay measurements. [17]

The user writes an input file containing the time since the end of bombardment (EOB) in days, hours, and minutes, as well as the net peak area or total number of counts under the peak of interest, and the total counting time. It also has a "control card" line in which the user writes the number of isotopes of interest (in this case two), the number of unknown half-lives (in this case one), and a number governing how far the iterations will proceed, called "CNV". The program is then run and outputs a list of calculated counts per minute, error, and the distance that the experimental data point is to the calculated fit point. It also states the forced half-life, error on the forced half-life, the counts per minute at end of bombardment, error, and decay factor. It also states what the fit of the calculated line is to the experimental data. The program takes in known half-lives of the isotopes, and iterates until it finds the best fit line to the data, changing the half-life if needed. The iteration is performed until the ratio of change of the decay constant to the standard deviation of the decay constant is less than the CNV number for all unknown half-lives. The program continues to iterate until In this case, it changed the value of the half-life of Nd-147 from 10.98 days as is published in Browne/Firestone to 11.308 days with error of 0.017 days. [8]

Figure 4.1 displays the experimental data showing the Nd-147 and Pm-147 decay data and its line as fitted by the Least Squares Method. It displays the counts per minute of Pm-147 as calculated by CLSQ. It also displays a calculated estimate of the amount of Pm-147 made from Nd-147 during the decay period.

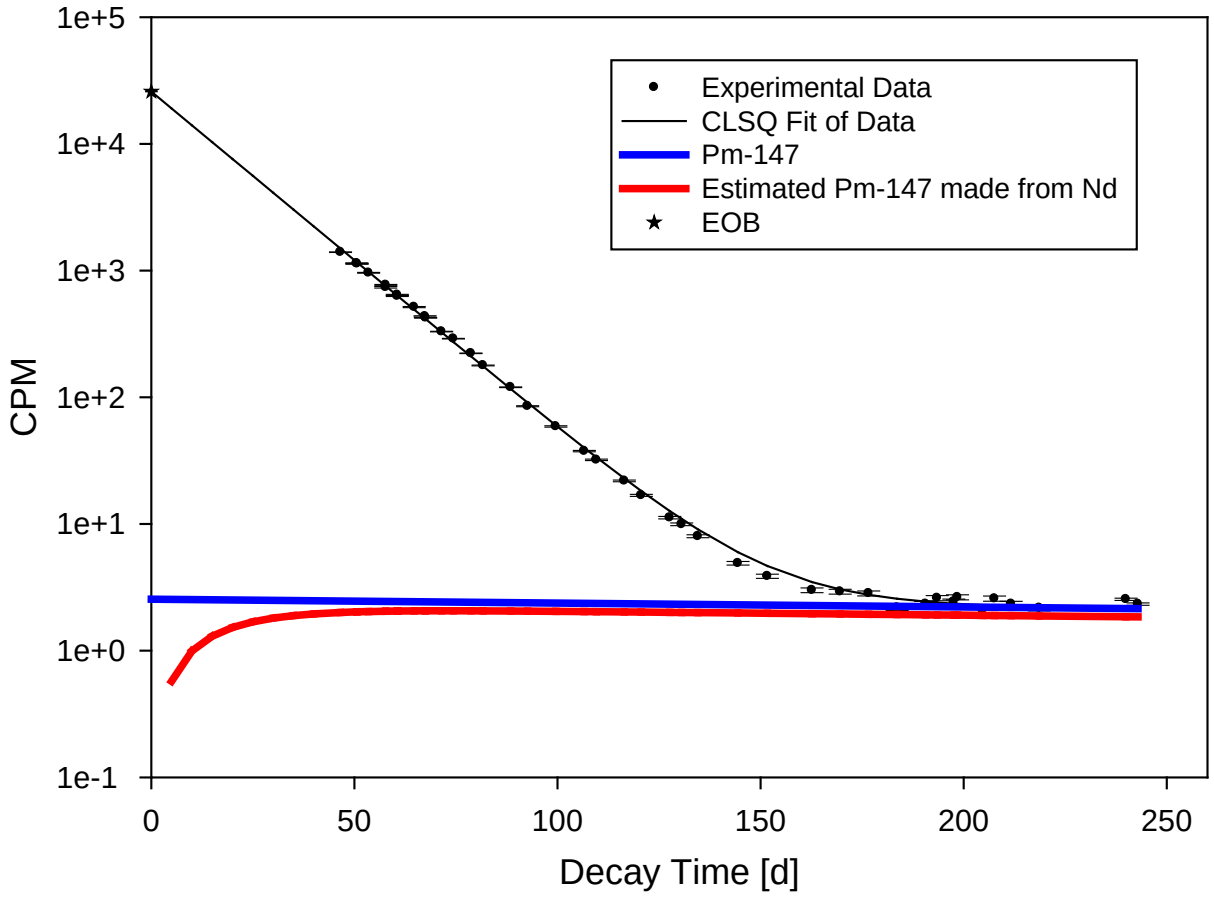

Figure 4.1: Cumming's Least Square Plot of Nd-147 to Pm-147 Decay

The curve that shows the calculated estimate of the amount of Pm-147 made from Nd-147 (C_{Pm-147}) during the decay period is calculated as follows:

$$C_{Pm-147} = \left(C_{Nd-147\,atEOB}\right)\left(\frac{\lambda_{Pm-147}}{\lambda_{Pm-147} - \lambda_{Nd-147}}\right)\left(e^{-\lambda_{Nd-147}*T} - e^{-\lambda_{Pm-147}*T}\right)(F) \qquad [4.1]$$

Where:

$C =$ Counts per minute

$$\lambda_{Pm-147} = \frac{\ln(2)}{2.62y * \frac{365.25d}{1y}} = 7.24E-3\frac{1}{d} = \text{ Decay Constant of Pm-147}$$

$$\lambda_{Nd-147} = \frac{\ln(2)}{11.308d} = 6.13E-2\frac{1}{d} = \text{Decay Constant of Nd-147}$$

$T =$ Decay Time

$$F = \frac{I_{Pm-147}}{I_{Nd-147}} = \frac{2.85E-3\%}{0.40\%} = 0.007125 = \text{Ratio of Intensities}$$

4.2 Isochain

Isochain is a java-based computer program that was used to estimate theoretical production of Neodymium-147 and Promethium-147 during and after irradiation of the Neodymium-146 sample. Its uses a library of isotopes of interest which utilizes known values for thermal and epithermal cross sections, half-lives, branching ratios for decay, and production products. It accepts input of the amount of nuclide(s) present in the initial sample (in user-chosen units of number of atoms, grams, Curies, or Becquerels), irradiation times, and flux ratio. It calculates data at a user-defined number of times. Table 4.1 contains the composition of the target NM-668, Table 4.2 contains the irradiation schedule of the target, and Figure 4.2 displays the chosen library of isotopes.

Table 4.1: Target NM-668 Neodymium Isotope Composition [10]

A of Nd Isotope	Assay Percent [%]	Amt of isotope [g]
142	0.43	4.0461E-06
143	0.29	2.7316E-06
144	0.7	6.6000E-06
145	0.69	6.5121E-06
146	97.46	9.2071E-04
148	0.32	3.0288E-06

150	0.13	1.2328E-06

Table 4.2: Target NM-668 Irradiation Schedule [21]

Time (s)	Time	# of Times	Flux	Flux Ratio
345600	96 hours	96	1.80E+15	30
2.16E+07	250 days	250	1	1
7.86E+07	910 days	100	1	1

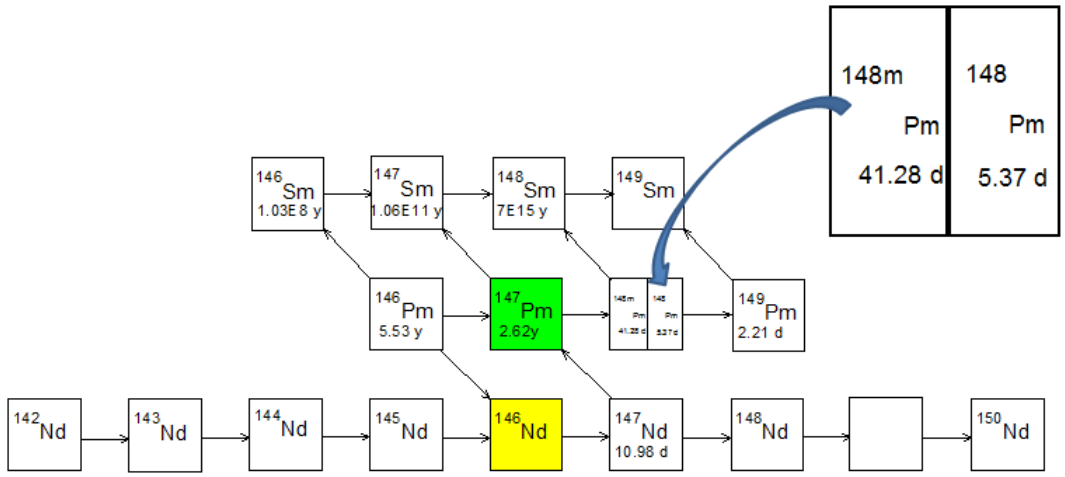

Figure 4.2: Library of Isotopes used in the Irradiation of NM-668 [16]

The sample NM-668 was irradiated for 96 hours in the Hydraulic Tube Position 3 which has a flux of 1.80E15 neutrons per second per square centimeter and a ratio of thermal flux to epithermal flux of 30. Isochain can also calculate the decay of radioisotopes after the sample is removed from the reactor. This feature is seen in the bottom two rows of Table 4.2. A low input number, 1, was chosen to represent the lack of neutron bombardment as an input of '0' would produce no output. Figure 4.3 below shows the results for production and decay of Nd-147 and Pm-147.

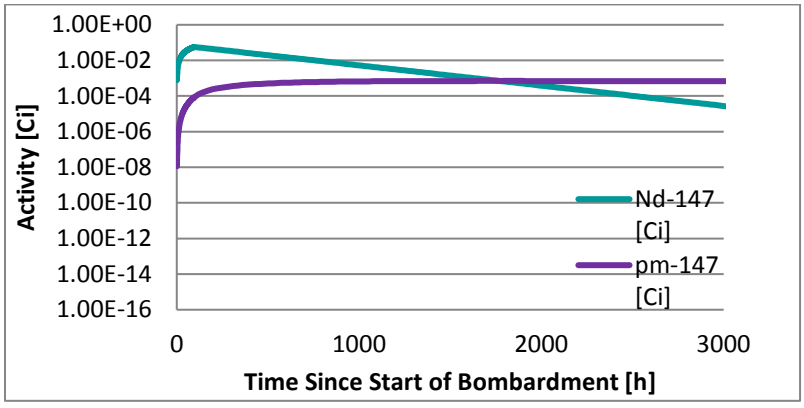

Figure 4.3: Theoretical Production and Decay of Nd-147 and Pm-147

5. Combining CLSQ and Isochain Results

In an effort to validate the CLSQ and Isochain code, the results from both programs were plotted on the same graph. In order to compare the results from both programs, results must be in the same units. A 'meet in the middle' approach of using units of gamma counts per second was utilized. As CLSQ uses experimentally obtained data, it contains data for two different nuclides, Nd-147 and Pm-147, both with different intensities. If CLSQ data would be converted to activity in order to compare it to the Isochain output, one would have to consider which point is which isotope when choosing which gamma intensity to use. If this were the case, the graph would be discontinuous. When the CLSQ output data is divided by the efficiency of shelf 20 (after normalizing all data taken at other shelves with the Geometrical Correction Factor), the data is in units of gamma counts per second. Isochain results were converted from an output in Curies to decays per second by multiplying by 3.7E10. Once in units of decays per second, the values are then multiplied by the intensity of the respected gamma, 0.4% for Nd-147 and 2.85E-3% for Pm-147, depending on which set of data used, to obtain the result in units of gamma counts per second. Due to the fact that 10% of the NM-668 sample was used to obtain counting data to as input into CLSQ, the results had to be multiplied by 10 in order to match the Isochain result, which estimated the production from the full sample, not 10% of the sample. This result is shown below in Figure 5.1.

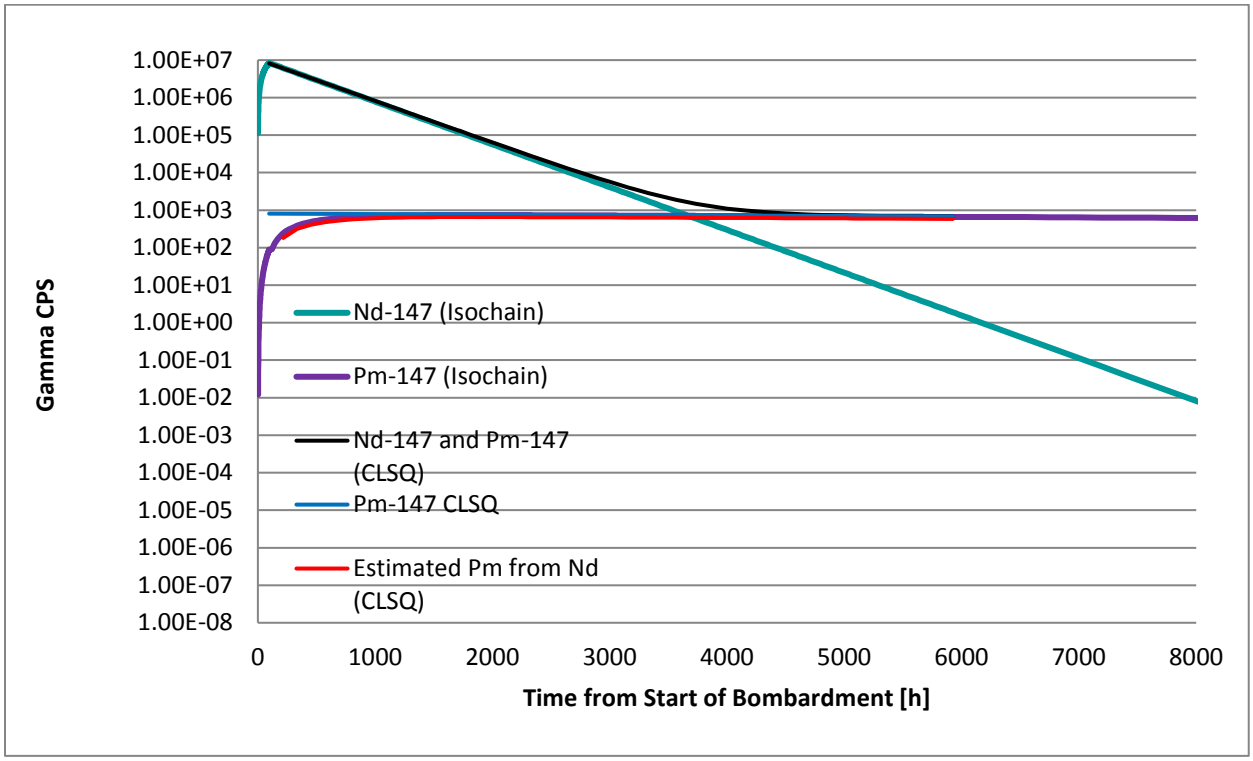

Figure 5.1: Combination of CLSQ Results and Isochain

5.1 Analysis of CLSQ and Isochain results

From a visual analysis of the CLSQ and Isochain combination plot, the two programs' results seem to agree with each other. Of particular interest in analysis are the points at the end of the bombardment and the location where the Pm-147 and Nd-147 lines intersect. Figure 5.2 below focuses on the beginning of bombardment to end of bombardment.

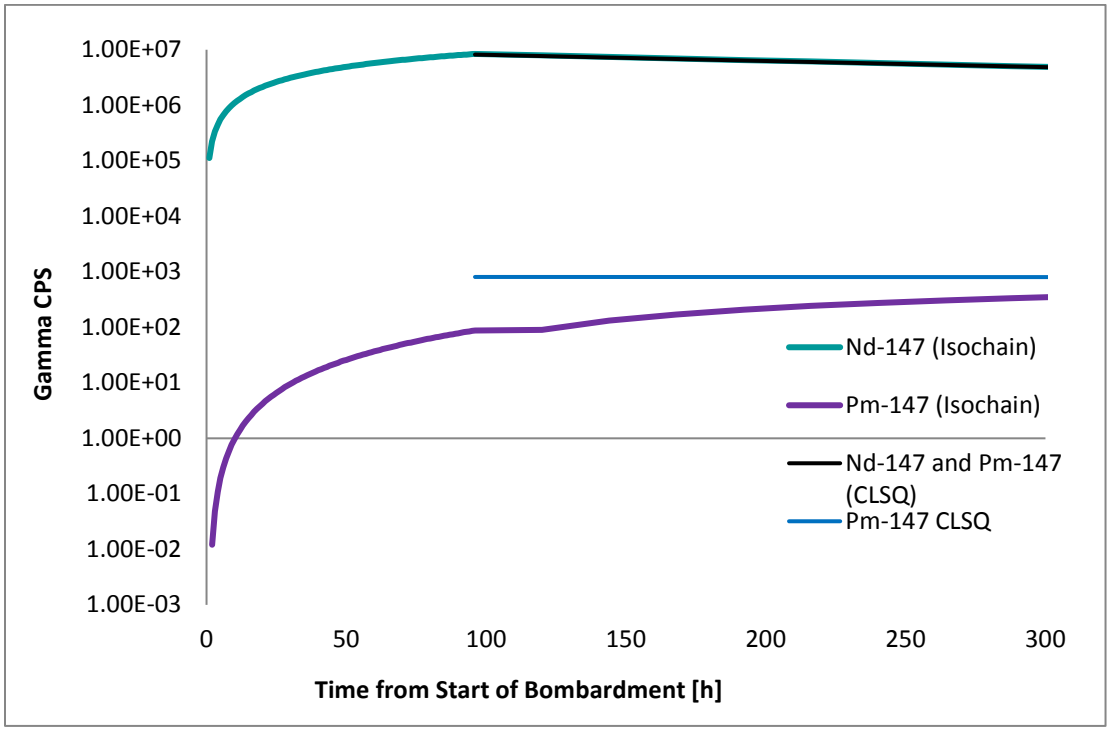

Figure 5.2: CLSQ and Isochain Plots at the Beginning and End of Bombardment

By extrapolation of the measured data, CLSQ estimated that there were 8.19E6 gamma counts per second at the end of bombardment, and Isochain estimated that there were 8.40E6 gamma counts per second at end of bombardment of Nd-147. The two separate calculations of the CPS at end of bombardment are extremely close, within of 2.6% of each other. From this evidence, Isochain accurately estimates the amount of Nd-147 produced in HFIR. Pm-147 is not produced as a direct result of bombardment, but as a decay product of Nd-147, which has a shorter half-life and a higher 120 keV gamma ray intensity than Pm-147. Thus, it takes longer to see the Pm-147 121 keV gamma ray via gamma counting. This is why CLSQ estimates the amount of Pm-147 present at the end of bombardment (807.5 gamma counts per second for the entire target) to be larger than the amount that Isochain estimates it to be (89.6 gamma counts per second) by a total of 89%. As time progresses, the Isochain estimate of the amount of Pm-147 created approaches the amount of Pm-147 measured by the detector and analyzed by CLSQ.

Another interesting point to analyze is the point where the amount of Pm-147 seen by the detector eclipses the amount of Nd-147 seen by the detector. This point of intersection is interesting because it illustrates how long the decay time must be for the Pm-147 to become useful as a quiet nuclear battery. This is shown below in Figure 5.3.

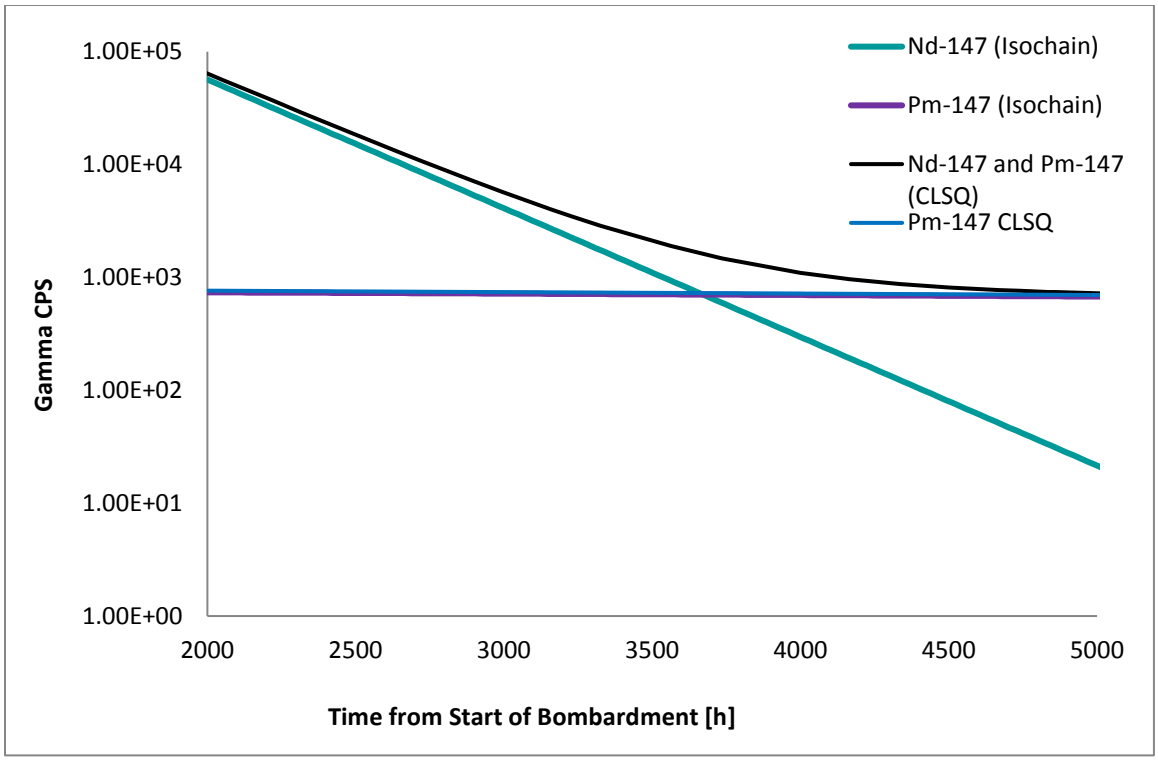

Figure 5.3: CLSQ and Isochain plots at the point where Pm-147 begins to be seen by gamma detection

Additional plots were produced using MS Excel in order to use the "Trendline" function and obtain best-fit equations to find the point of intersection. Using data from CLSQ, a plot was made using the straight portion of the Nd-147 decay line and the Pm-147 estimation line. The Nd-147 best fit line was used to extend the plot past the intersection point in order to see the intersection. As shown in Figure 4.1 above, the error is small and difficult to see with the size of the points on a graph. This is seen below in Figure 5.4.

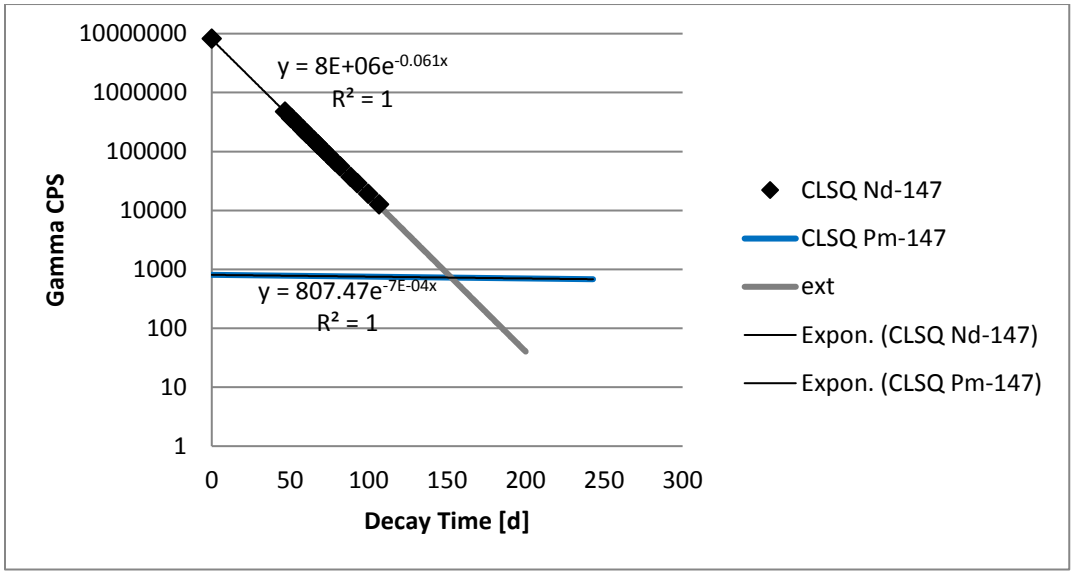

Figure 5.4: Intersection of Nd-147 and Pm-147 in Gamma CPS

In order to find the exact time post bombardment when the intersection occurs, the two best fit lines were set equal to each other and solved for x:

$$807.47e^{-(7E-4)*x} = (8E6)e^{-0.061*x} \quad [4.2]$$

$$e^{-(7E-4)*x+0.061*x} = 9907.49 \quad [4.3]$$

$$e^{0.0603x} = 9907.49 \quad [4.4]$$

$$\ln 9907.49 = 0.0603x \quad [4.5]$$

$x = 153$ days after EOB

From this equation, it is seen that it takes 153 days for the Nd-147 to decay to the point where Pm-147, with its weaker gamma ray, can be seen via gamma spectroscopy. This amounts to about 13.5 times the 11.308 day half-life (according to CLSQ) of Nd-147.

This particular result from the CLSQ analysis is compared to the intersection of the Isochain-produced estimates for production of Nd-147 and Pm-147. The isolated points of interest are shown below in Figure 5.5.

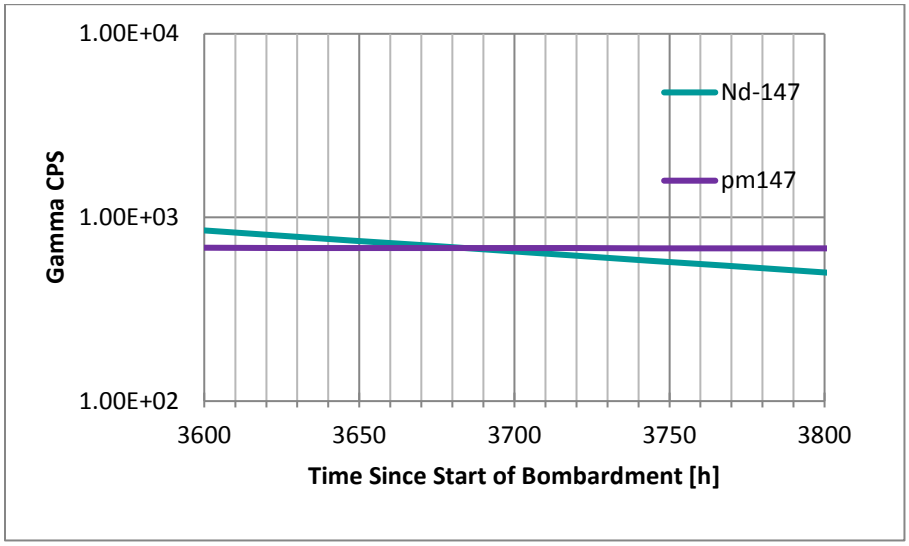

Figure 5.5: Isochain-Produced plot of Nd-147 and Pm-147 in units of Gamma CPS

In order to approximate the time of intersection, the two lines were plotted and zoomed in to enable seeing the intersection more closely. From a visual inspection of the graph, intersection happens at x=3680 hours after the start of bombardment, or 3584 hours (149 days) after the end of bombardment. This amounts to a 2.6% difference.

Another interesting analysis is to determine when the point of intersection using the Isochain output in Curies, before converting it to Gamma counts per second in order to compare to CLSQ. It is expected that the intersection will happen before the intersection in units of

gamma counts per second due to the higher intensity of the Nd-147 characteristic gamma ray. This higher intensity allows it to dominate the experimental analysis performed by gamma spectroscopy. Promethium-147 has a much lower intensity so it will not be seen by a gamma spectrometer when it first starts to grow in but that does not mean that it does not dominate in terms of amount of activity. Figure 5.6 focuses on the region of intersection of the Isochain-produced plot of Nd-147 and Pm-147 in Activity units. From graphical analysis, it is observed that intersection happens at approximately 1750 hours since the start of bombardment, or 1654 hours (69 days) since the end of bombardment.

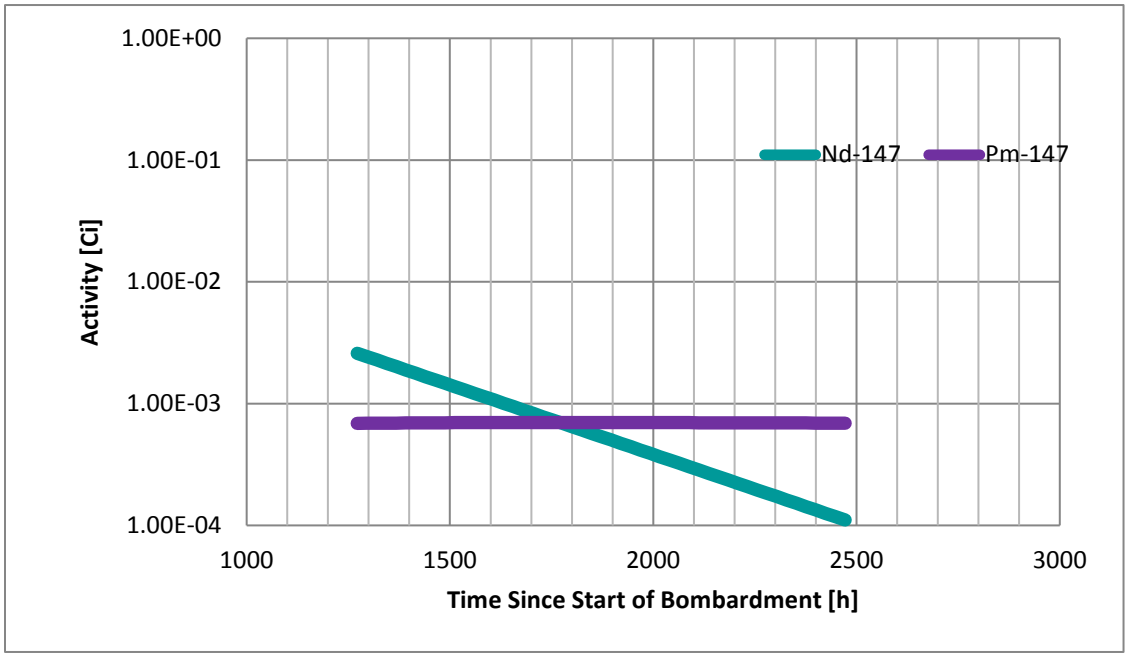

Figure 5.6: Isochain-Produced plot of Nd-147 and Pm-147 in units of Curies

6. Preparation of the Pm-147 Target for further irradiation

A sample of Pm-147 prepared by Rose Boll in 2006 was used to prepare Sample NM-784 in order to determine the neutron absorption cross section of Pm-147. This is a different sample than NM-668 mentioned above. The new sample was evaporated to dryness on a hotplate in a scintillation vial in December 2012. It was then rewetted to clean the sides of the scintillation vial with 0.5mL of 10M HCl and evaporated to dryness again. This produced 4.60 counts per second of Pm-147's characteristic gamma ray of 121 keV. Activity was calculated by dividing the counts per second by the intensity of the gamma ray in question and then again by corresponding shelf efficiency of the detector in question, as shown in Eq.6.1:

$$Activity[Ci] = \frac{4.60cps}{\frac{2.85E-5}{2.10E-2}} = 7.69E6dps * \frac{1\mu Ci}{37000dps} = 207.73\mu Ci \qquad [6.1]$$

There was rust on the automatic pipette which contaminated the sample with iron during the transfer from the original bottle to the hotplate. This was easily corrected with an MP-1 column prepared with 3 mL bed volume MP1 resin with a mesh size of 200-400 in chloride form. The

iron rust “stuck” to the column, allowing the Promethium flow through the column in a clear solution to be evaporated to dryness. This yielded a total of 194.4 µCi of Pm-147.

6.1 LN Separation Columns

At this point in the target preparation, the sample still had some of the original Neodymium-146 target in it. This is considered an impurity and can be seen as a white residue when the sample is evaporated to dryness. In order to remove this impurity, a series of LN columns were used. The first column utilized a 3mL bed volume, 14 cm high column with LN B50-A resin in 0.5M HCl. The results are shown below in Figure 6.1:

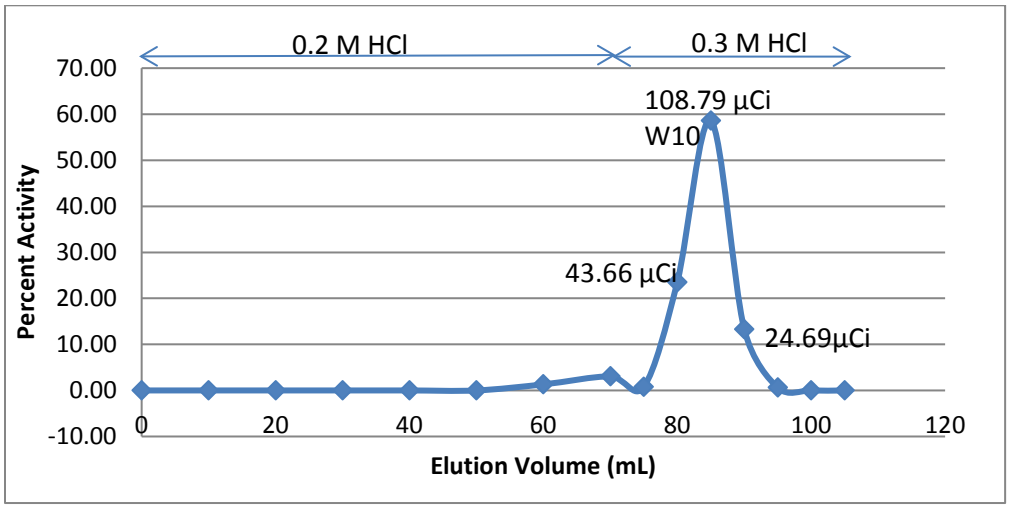

Figure 6.1: First B50-A Resin LN Separation Column, 3 mL Bed Volume

Washes W9, W10, W11 contained 43.66 µCi, 108.79 µCi, and 24.69 µCi of Pm-147, respectively, for a total of 177.14 µCi. The washes were then combined and evaporated to dryness which yielded a total of 171.41 µCi of Pm-147, with a small amount of activity being lost due to transfer. Upon dryness, the sample still had a white residue, which was most likely due to presence of the original target. The sample was then oxidized with five drops of HNO_3 and then three drops of H_2O_2 and evaporated to dryness again. Figure 6.2 below shows the reduction of Neodymium-146 seen in the form of a white residue that the oxidation produced.

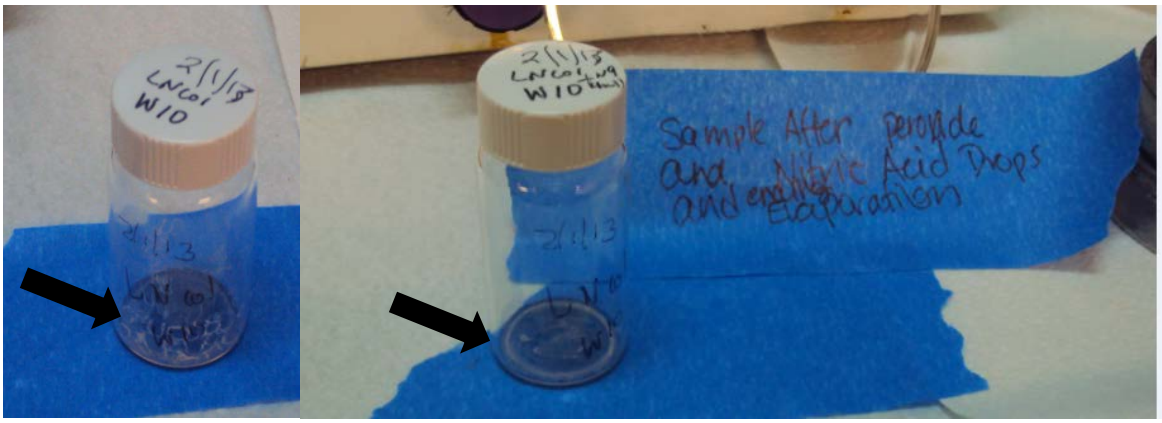

Figure 6.2: Before and After the HNO_3 and H_2O_2 Oxidation Procedure

This yielded 191.45 µCi of Pm-147. A larger amount of Pm-147 was seen due to less self-shielding in the sample due to the absence of the material that was oxidized off. However, this did not provide the desired improvement of a significant reduction in the amount of white residue seen. Another LN column, using the same column setup as in the first run, was used after rewetting the sample with approximately 3 mL of 0.2M HCl. The sample was heated slightly to get the sample to dissolve then transferred to the column via pipette. The bottle was rinsed to ensure that the entire sample was put onto the column. The results are shown below in Figure 6.3:

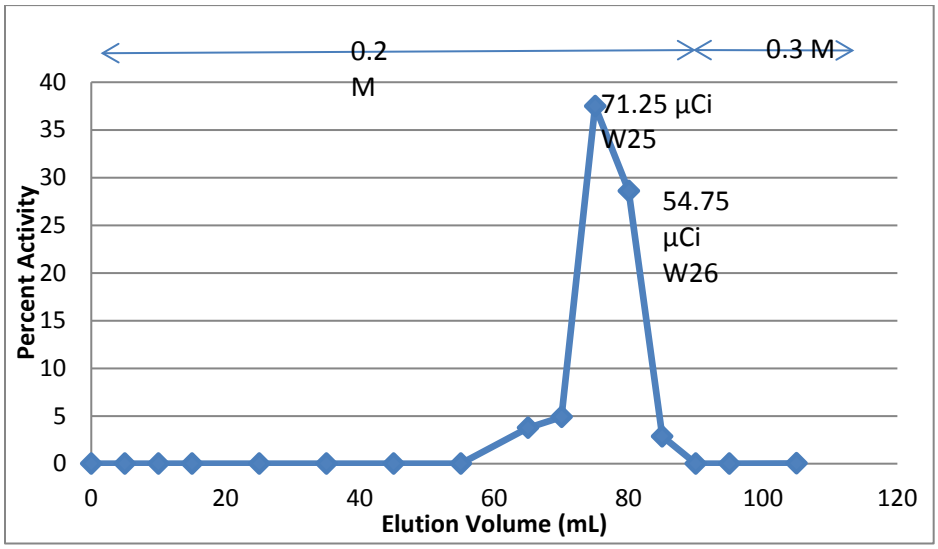

Figure 6.3: Second B50-A Resin LN Separation Column, 3 mL Bed Volume

Washes W25 and W26 contained 71.75 µCi and 54.75 µCi of Pm-147, respectively. Figure 6.4 below shows the improvement in the appearance of the sample, with the goal of eliminating the white Nd-146 residue. Upon visual inspection, it was determined that no Nd-146 residue could be seen, and that the amount of Nd-146 left, in any, was satisfactory for the purpose of irradiation of the target in HFIR.

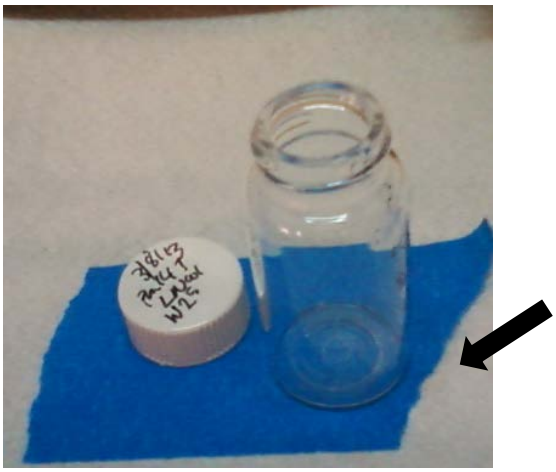

Figure 6.4: Combined Washes W25 and W26 Evaporated to Dryness

6.2 Loading of Material into Quartz Ampoules

The sample was placed inside a Suprasil synthetic quartz ampoule that had been cleaned in order to reduce the chance of cross-contamination. This ampoule had a 'neck' put into it with an opening just large enough to squeeze a small pipette tip so as to aid in the sealing process. In order to prepare the ampoule for use, it was first rinsed with 16M HNO_3 three times and then rinsed with de-ionized water and placed in a beaker to hold it upright. Then, it was placed in a laboratory oven for 30 minutes at 110 ± 5°C for 30 minutes and then in a desiccator to dry using filtered air overnight.

The dry sample containing Washes W25 and W26 was then rewetted with a total of 300 µL of 1.2M HNO_3.to aid in getting all of the residue to the bottom of the vial. The sample was then evaporated to dryness and then rewetted with a known volume of 50 µL of 1.2M HNO_3 and placed in a small plastic vial with a purple top. The extra rewetting and evaporating step was done to make the sample have a smaller volume, thereby enabling to a new vial. This yielded a total of 129.15 µCi of Pm-147 in solution in the plastic vial. Five microliters of this solution were removed and placed in a separate vial with 95 µL of 0.1M HNO_3 and sent for mass spectrometry. The remaining 45 µL were placed in the previously cleaned synthetic glass quartz vial and the plastic vial was rinsed with 50 µL of 1.2M HNO_3 and let sit. The solution in the quartz vial was then dried with forced and filtered air. The final amount from the plastic vial was then transferred to the quartz vial and dried with forced and filtered air. It was then counted and showed to contain 108.38 µCi of Pm-147. It was then handed off to a technician to be sealed.

During the sealing process, the ampoule broke. In order to recover the sample, 75 µL of 1.2M HNO_3 was placed into the bottom of the broken ampoule and let sit on top of a Kim-wipe in a scintillation vial in order to dissolve the dried sample and allow for transfer to a new quartz vial. A new, and slightly thicker, synthetic quartz vial was cleaned by the method mentioned above. The solution from the broken quartz bottom was removed via pipette and placed in the new quartz vial and counted. No counts from Pm-147's 121keV gamma ray were seen, so 75 µL

of 8M HNO_3 was placed in the broken quartz bottom and left to sit overnight to dissolve the remaining solids. This solution was transferred to the new quartz vial and the solution was counted and showed 4.24 µCi of Pm-147. The broken ampoule was rinsed again with 75 µL of 1.2M HNO_3 and transferred to the new ampoule and placed this under the air to dry. The rinsed ampoule bottom was counted and no counts at 121 keV were seen.

As it turned out, there was a crack in the broken ampoule that let the solution and the sample out into the Kim-wipe that it was sitting in. The Kim-wipe paper was dissolved in 3 mL of 96% concentrated Suprapur H_2SO_4 in a beaker on a hotplate. A total of 45 drops of H_2O_2 was added to this mixture in order to remove the carbon from the paper. This turned the solution dark brown then to amber and then back to dark brown again. Then, 3 mL of 8M HNO_3 was added, turning the solution yellow. The broken glass vial bottom and the scintillation vial it was sitting in were rinsed with 1mL 8M HNO_3 and that solution was added to the beaker on the hotplate. Another 13 drops of 30% H_2O_2 was added to this solution and transferred to a scintillation vial. The beaker was rinsed with de-ionized water and the beaker was put on the hotplate to evaporate to dryness. Because the Pm-147 was recovered from a KimWipe, contaminates were introduced from the dissolved paper, and further separations were required to purify the Pm-147 target again.

6.3 AG50 Separation Column

An AG50 column with a 1mL bed volume was prepared. The purpose of using AG50 resin is to retain the Pm-147 while allowing the sulfate that was introduced in the paper dissolving process to go through the column. The first AG50 column did not retain the Promethium as expected so the fractions were re-combined into a larger beaker to prepare a more dilute solution. These fractions were evaporated to dryness and 2 mL of HNO_3 and 0.5 mL of H_2O_2 was added to the beaker. In order to dilute the solution, 10 mL of de-ionized water was added to the column.

The second AG50 column was prepared with a 2 mL bed volume and conditioned with 6 mL of 8M HNO_3 and then rinsed with de-ionized water. The solution was loaded onto the column in fractions. It was stripped with 8M HNO_3 and rinsed with de-ionized water twice. The first strip yielded 58.33 µCi of Pm-147 and the following rinse yielded 17.89 µCi µCi of Pm-147. The second strip with 8M HNO_3 yielded µCi of Pm-147. These were combined into a scintillation vial and evaporated to dryness. There was a yellowish residue at the bottom of the scintillation vial so 10 drops of H_2O_2 were added to the vial along with 1 mL of HNO_3, and 10 more drops of H_2O_2. This was evaporated to dryness to produce a less yellow residue than before. This was subsequently counted, and it was determined that 97.16 µCi of Pm-147 was recovered during this process.

The sample was rewetted with 500 µL of 1.2M Nitric Omni trace acid to transfer to another small plastic purple top vial. The scintillation vial was rinsed with 100 µL of 1.2 M Nitric Omnitrace acid. The sample in the purple top vial was left to dry overnight under forced and filtered air. Then, a total of 100 µL of 1.2 M Nitric Omnitrace acid was added to the dried sample and transferred to the new and thicker synthetic quartz ampoule. After two rinses of the purple vial, a wet gamma count of the quartz ampoule showed a total of 73 µCi of Pm-147. After some more acid was added to the ampoule to aid in moving all of the Promethium to the

bottom, it was dried using forced and filtered air. A gamma count of the dried sample revealed 97 µCi of Pm-147, equivalent to 1.045E-4 mg as shown in the calculation below:

$$\lambda_{147} = \frac{\ln 2}{2.62y * 365.25d/y * 24h/d * 3600s/h} = 8.383E-9\frac{1}{s}$$

$$A = \lambda_{147} N \rightarrow N = \frac{A[dps]}{\lambda_{147}} = \frac{97\mu Ci * \frac{1Ci}{1E6\mu Ci} * \frac{3.7E10dps}{1Ci}}{8.383E-9\frac{1}{s}} = \frac{3.589E6dps}{8.383E-9\frac{1}{s}}$$

$N = 4.28E14$ disintegrations in sample

$$Mass_{147} = 4.28E14d * \frac{1mol}{6.02E23} * \frac{147g}{mol} * \frac{1000mg}{1g} = 1.045E-4mg$$

The quartz ampoule was then successfully sealed shut in a glovebox, ready to be loaded into an aluminum target capsule. Figure 6.5 shows the quartz ampoule in the chuck that was used to successfully seal it shut.

Figure 6.5: Sealed Quartz Ampoule

6.4 Aluminum Capsule Loading

A pre-made aluminum target "rabbit" was chosen from the Nuclear Medicine Group's supply. Figure 6.6 shows a diagram of a typical rabbit.

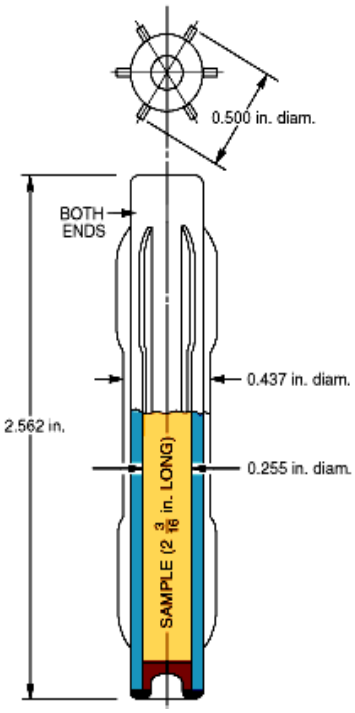

Figure 6.6: Hydraulic Tube Capsule Assembly, Courtesy of ORNL Website: http://neutrons.ornl.gov/facilities/HFIR/ [13]

The aluminum target selected was pre-labelled "NM-784". Quartz wool was placed at the bottom of the target to serve as a cushion to keep the sample in place. The quartz ampoule was then wrapped in aluminum foil and carefully placed into the target. Quartz wool was then placed on the top of the sample.

6.5 Welding of Aluminum Targets

A certified welder used a tungsten inert gas welder to weld the aluminum end cap to the target, sealing the sample inside the target. A weld inspection report was generated as required to certify the target for irradiation inside HFIR.

6.6 Testing and Certification of the Promethium-147 Target

In order to ensure integrity of the target inside the reactor, the target was subjected to two helium leak tests and one hydrostatic pressure test.

6.6.1 Helium Leak Test

Two helium leak tests were performed using the bell jar technique, one before and another after the hydrostatic pressure tests in order to assure weld integrity. In order to be used in HFIR, the leak rate should be no larger than 1.0E-7 standard cubic centimeter per second. The leak rate observed in both tests was 2.18E-8 standard cubic centimeter per second.

6.62 Hydrostatic Pressure Test

A hydrostatic pressure test was performed in order to ensure that the capsule NM-784 could withstand the conditions that it would be subjected to in the reactor. Two 15 minute tests were performed. The capsule was loaded into a pressure chamber, filled with water and pressurized using a hand pump to 1040 psi both times. The capsule was weighed before and after the test to make sure that it did not take on any weight from the pressurized water. It remained the same mass, 8.732 grams, and as a result, it passed the hydrostatic pressure test. After the tests were completed, a radiograph was taken of the target and is shown below in Figure 6.7.

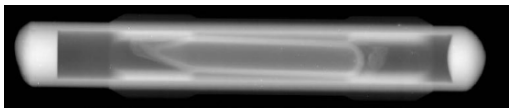

Figure 6.7: Radiograph of Target NM-784

6.7 Irradiation of the Promethium Target

Oak Ridge National Laboratory's (ORNL) High Flux Isotope Reactor (HFIR) is used for numerous experiments and isotope production. Built in the mid-1960's it is an 85 MW reactor. It is the highest flux reactor-based source of neutrons for research in the United States. HFIR is a beryllium-reflected, light-water-cooled and -moderated, flux-trap type reactor that uses highly enriched uranium-235 as the fuel. [13] The Hydraulic Tube is often used in experiments because targets can be inserted and removed while the reactor is still on-line. Figure 6.8 shows the reactor core assembly, showing the flux trap that contains the target bundle.

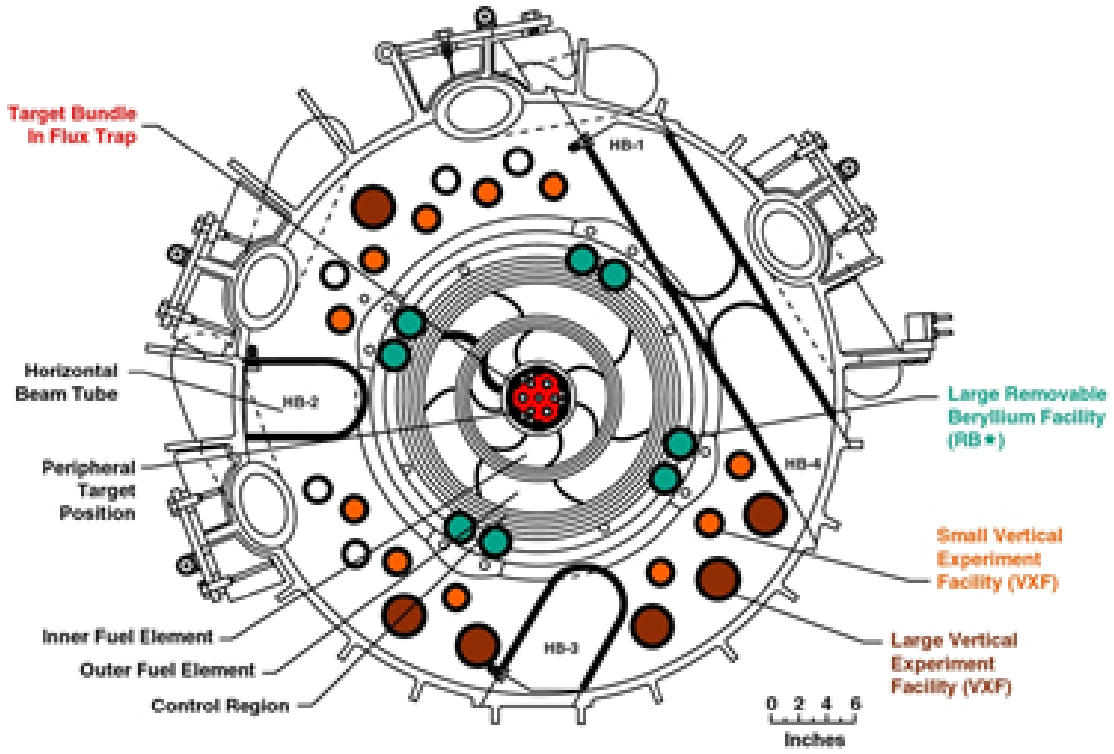

Figure 6.8: Reactor Core Assembly, Courtesy of ORNL Website: http://neutrons.ornl.gov/facilities/HFIR/ [13]

The center of the reactor core is the flux trap where the fuel region surrounds the center containing the targets. This configuration allows fast neutrons from the fuel to be moderated in the target region, thus producing a high thermal neutron flux at the center. Figure 6.9 shows this more clearly.

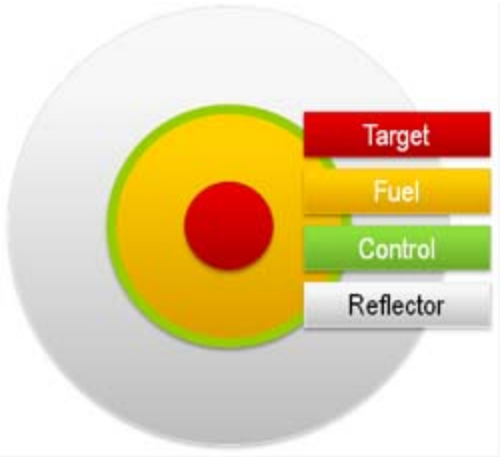

Figure 6.9: HFIR Reactor Core Diagram, Courtesy of ORNL Website: http://neutrons.ornl.gov/facilities/HFIR/ [13]

Figure 6.10 below shows the location of the Hydraulic Tube ('HT') that is used in the experiment.

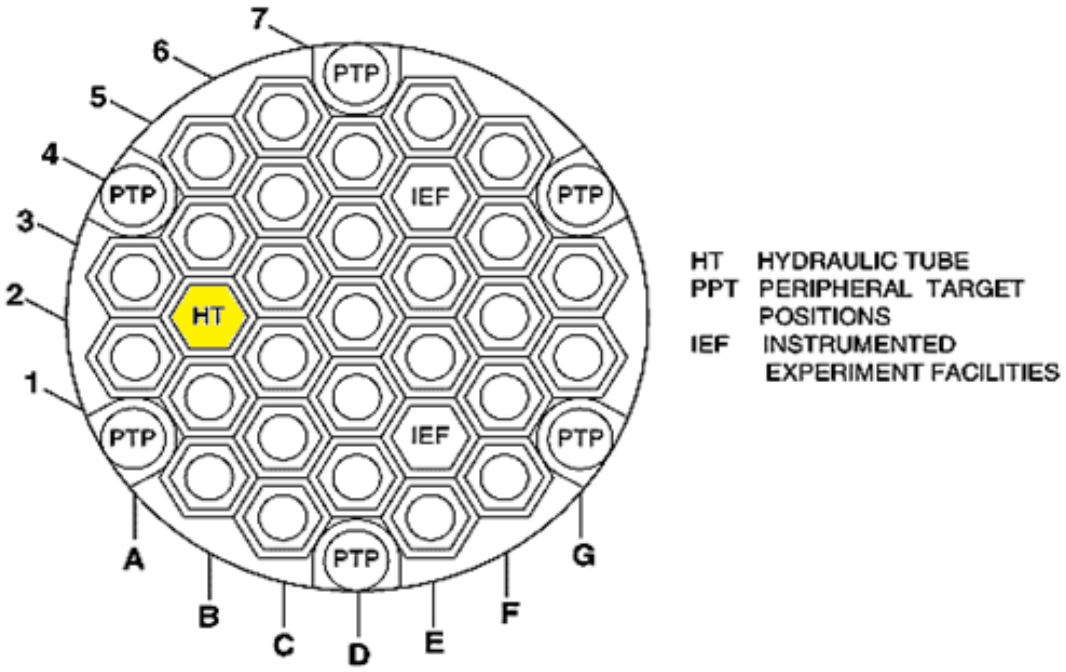

Figure 6.10: Target Loading in the Flux Trap, Courtesy of ORNL Website: http://neutrons.ornl.gov/facilities/HFIR/ [13]

6.8 Irradiation Schedule

The sample NM-784 with 97 μCi of Pm-147 was inserted into the hydraulic tube's position 5 during HFIR's Cycle #448. The experimentally determined flux for this position is 2.05E15 neutrons per second per square centimeter and the epithermal flux is 7E13 neutrons per second per square centimeter [14]. The experimentally determined flux ratio of thermal flux to epithermal flux for this position is 30. It was desired that 100 μCi of Pm-148 ground state (half-life 5.370 days) and 10 μCi of Pm-148 metastable state (half-life 41.29 days) be created in the reactor. Isochain was used to determine the amount of reactor time needed. According to the calculation and in order to produce 100 μCi of Pm-148 ground state, 6.25 hours of reactor time was needed, and in order to produce 10 μCi of Pm-148 metastable state, 8.5 hours of reactor time was needed. The longer amount of time was chosen to ensure satisfactory amounts of both were produced and then rounded up to 10 hours to add a margin of safety in the time needed. Target NM-784 started irradiation in HFIR Hydraulic Tube position #5 on July 6, 2013 at 11:30 am and finished at 9:30 pm on that same day.

In order to check the calculation done with Isochain, a rough calculation was done by hand. This calculation neglected the burnup of Pm-148 ground and metastable states. The following equation was used to estimate the minimum time required in the reactor:

$$A_{148} = N_{147}\sigma_{eff}\phi(1 - e^{-\lambda_{148}t_{ir}}) \qquad [6.2]$$

Where:

A= Desired Radioactivity

N= Number of Atoms in Target= $\frac{A_{147}}{\lambda_{147}} = \frac{97\mu Ci * \left(\frac{1Ci}{1E6\mu Ci}\right) * \left(\frac{3.7E10}{1Ci}\right)}{\frac{\ln(2)}{2.62y * (365.25d/y) * (24h/d) * (3600s/h)}} = 4.281E14 atoms$

ϕ =Thermal Flux of the HFIR's Hydraulic Tube Position #5=2.05E15neutrons/cm^2*s

λ_{148g} = Decay Constant of Pm-148 ground state=5.378E-3 1/hour

λ_{148m} = Decay Constant of Pm-148 metastable state= 6.99E-4 1/hour

t_{irr} = Irradiation Time (unknown)

And:

σ_{eff} =Effective Cross Section = $\sigma_{th} + \frac{\sigma_{epi}}{(th/epi)}$ [6.3]

Where:

σ_{th} = Thermal Cross Section

σ_{epi} = Epithermal or Resonance Cross Section

th/epi = Thermal Flux to Epithermal Flux Ratio of HFIR Hydraulic Tube position #5= 30

Table 6.1 below shows the cross sections used in the calculations

Table 6.1: Cross Sections [12]

	σ_{th} [b]	σ_{epi} [b]	σ_{eff} [b]	σ_{eff} [cm^2]
Pm-147^g	96	1274	138.5	1.39E-22
Pm-147^m	72.4	790	98.7	9.87E-22

The calculation performed using Equation 6.2 and data above resulted in 5.75 hours of irradiation needed to obtain 100 μCi of Pm-148g and 0.6113 hours of irradiation needed to produce 10 μ Ci of Pm-148m. This differs from the Isochain calculation of 6.25 hours needed to produce 100 μCi of Pm-148g and 8.5 hours needed to produce 10 μCi of Pm-148m. This vast difference is due to the fact that Isochain takes into account the burnup of Pm-148 ground and metastable states during the course of the bombardment. This quick calculation did not take into account this burnup.

7. Analysis of the Promethium Target

The target was received from HFIR and cut open on July 9, 2013. The ampoule was cleaned the next day by using an 8M HNO_3 bath and 2 rinses with de-ionized water. It was then placed in a plastic bottle and crushed. After adding 0.5 mL 8M HNO_3 to the bottle and agitating it to dissolve the solids, it was transferred by pipette to a labeled scintillation vial and placed on a hotplate to evaporate to dryness. One mL of nitric acid was added to the scintillation vial again and 20μL (2% of the total solution) was removed and put into a smaller vial in order to be counted.

7.1 Radioactivity Measurement

The samples were counted and recorded. Four peaks were chosen, representing different nuclides of interest, as seen below in Table 7.1.

Table 7.1: Nuclides of Interest [8]

Nuclide	Half-Life [d]	Peak [keV]
Pm-149	2.117	286.03
Pm-148	*	550.274
Pm-148m	41.29	629.62
Pm-148g	5.370	1465.12

*This energy is representative of both states.

These peaks were chosen due to their higher intensities. The results from the gamma counting were run through CLSQ to calculate a fitted line, and an estimate of the counts per minute at the end of bombardment. The graphs are shown below in Figures 7.1-4. In these graphs, the CLSQ-provided error is plotted but is very small it is almost not visible on the plot.

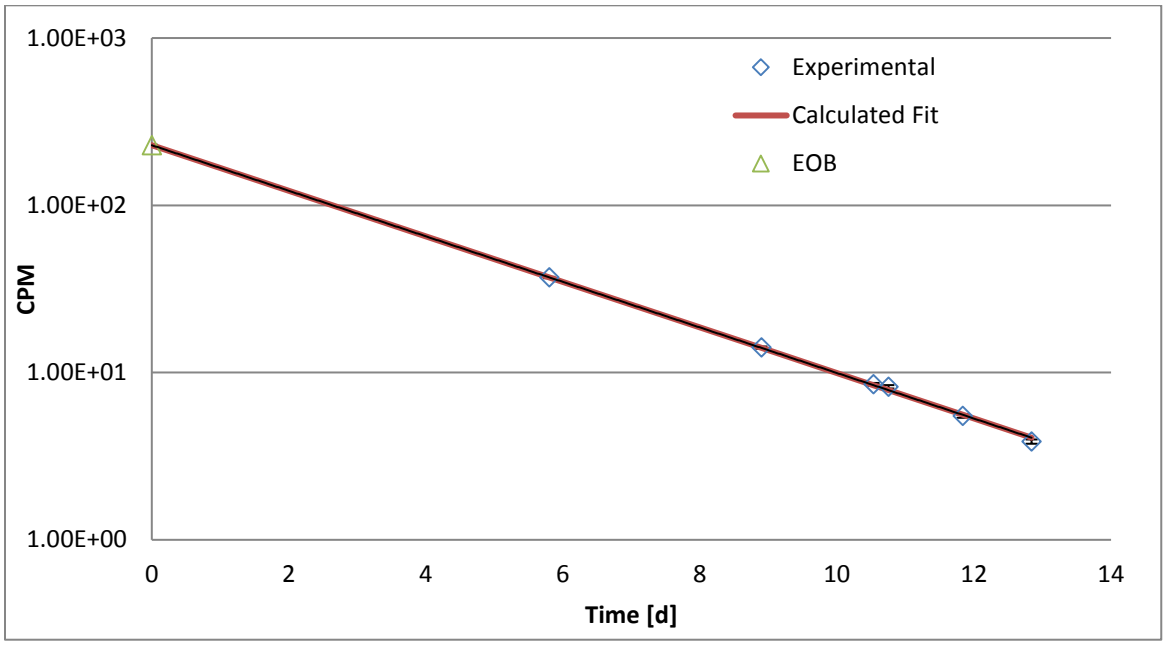

Figure 7.1: Promethium-149 (286.03 keV)

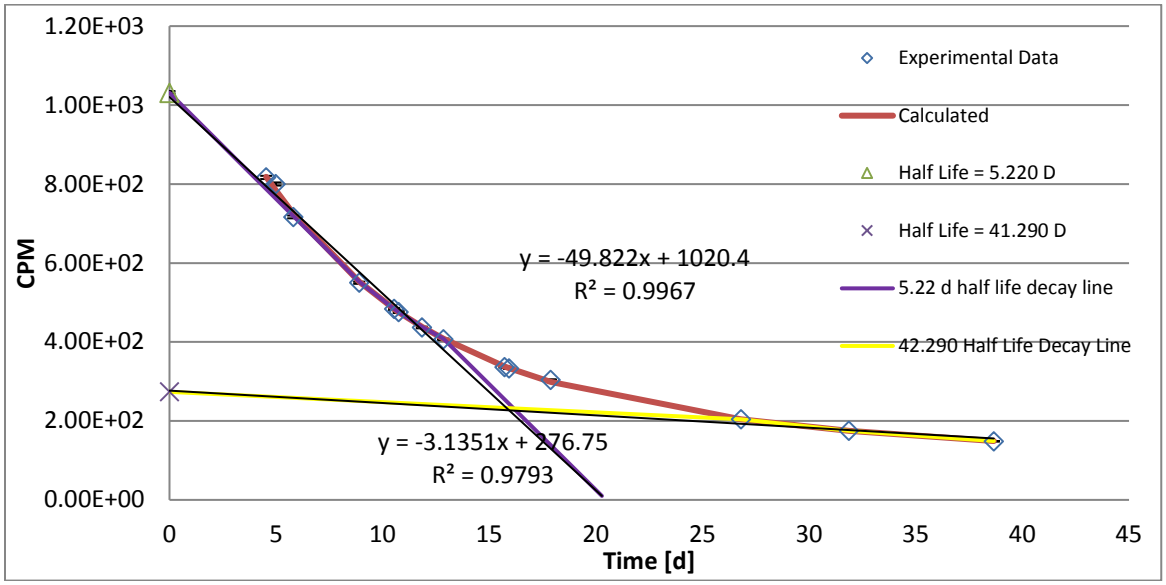

Figure 7.2: Promethium-148 (550.274 keV)

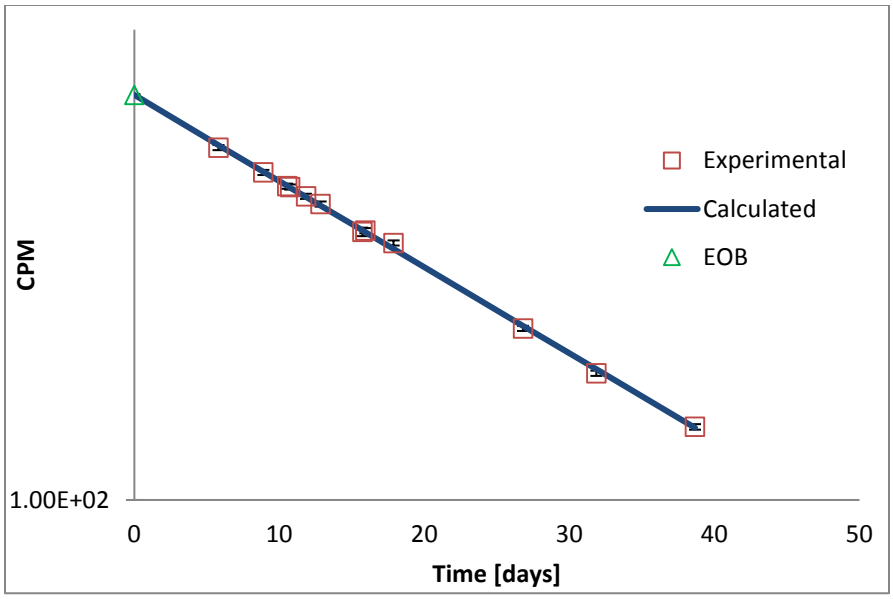

Figure 7.3: Promethium-148m (629.62 keV)

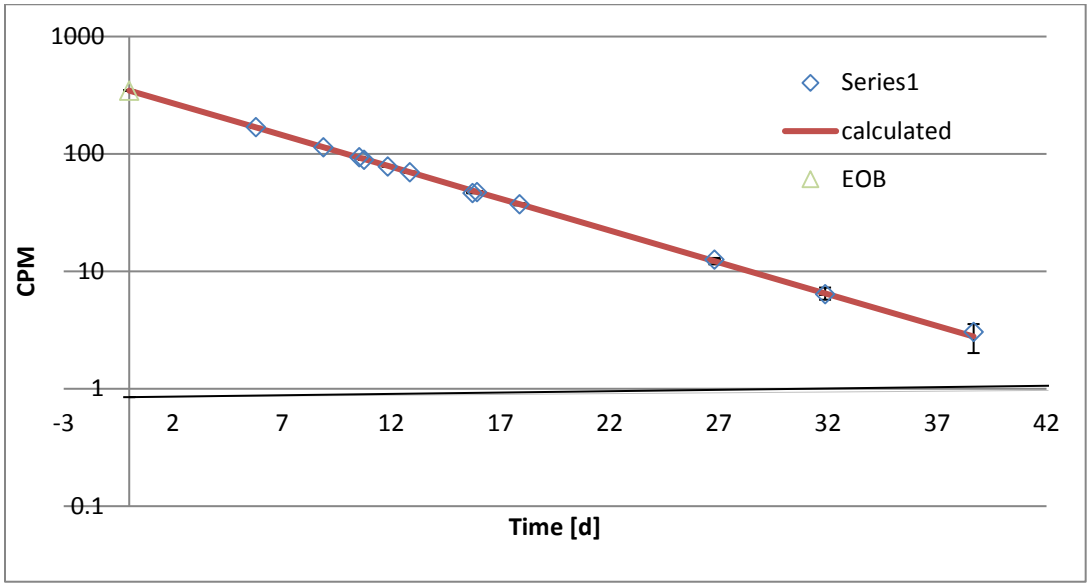

Figure 7.4: Promethium-148m (1465.12 keV)

The Activity at EOB is calculated by Equation 7.1 and is tabulated for all four nuclides of interest in Table 7.2 below.

Table 7.2: Activity at End of Bombardment

Nuclide	CPS at EOB [cps]	Effciency	Gamma Intensity	Activity at EOB [dps]	Activity at EOB [µCi]	A: DPS in entire sample NM-784
Pm-149	3.81	0.001835100	0.0285	72880.3	1.970	3.64E+06
Pm-148m	3.67	0.000865860	0.886	4783.9	0.1293	2.39E+05
Pm-148g	5.78	0.000372680	0.222	69801.2	1.887	3.49E+06

The output from CLSQ is given in counts per minute and is then converted to counts per second by dividing by 60. The activity of the counted sample is calculated by the below equation:

$$A = \frac{[CPS]}{E/I} = [dps] \quad [7.1]$$

Where:

E= Effciency of the Detector Shelf that sample was placed on for the Gamma Energy of interest

I= Intensity of Gamma photon [8]

The efficiency of the detector is calculated by ORNL personnel using a multi gamma standard and is kept for future experimenters to use. It combines the geometric efficiency of the detector (based on the distance between the detector and the source) and the intrinsic efficiency of the detector. Dividing the counts per second by the detector efficiency yields the number of gamma counts per second that are being emitted by the source. The activity in decays per second is then obtained by dividing that result by the intensity of that particular gamma-ray photon. The activity is then converted to microcuries:

$$A = [dps] * \frac{1Ci}{3.7E10dps} * \frac{1E6\mu Ci}{1Ci} = [\mu Ci] \quad [7.2]$$

Because only 2% of sample NM-784 was actually counted in the detector, it is necessary to divide the EOB activity obtained by CLSQ by 0.02. It is assumed that the entire sample will behave as the 2% that was counted. These calculations are tabulated in Table 7.2 above and are used to calculate the cross section of Promethium-147 to both the ground and metastable states of Promethium-148 below.

7.2 Promethium-147 Cross Section Calculation

First, a rough cross section calculation was done, similar to what was done previously in section 6.8. This rough calculation does not take in to account the burnup of the Pm-148 ground and metastable states that are produced in the reactor and thus production of Pm-149. The result of the calculation is to determine the effective cross section an irradiation of 10 hours. Due to this experiment, the thermal and epithermal cross sections cannot be distinguished. Again, the equation is:

$$A_{148} = N_{147}\sigma_{eff}\phi(1 - e^{-\lambda_{148}t_{ir}}) \quad [7.3]$$

$$3.49E6dps = (4.281E14atoms) * \sigma_{eff Pm-147^g} * \left(2.05E15\frac{n}{cm^2 * s}\right)(1 - e^{-(5.378E-3\frac{1}{h})*10h}) \quad [7.4]$$

$$3.977E-24cm^2 = \sigma_{effPm-147^g} * (1 - e^{-(5.378E-2)}) \quad [7.5]$$

$$3.977E-24cm^2 = \sigma_{effPm-147^g} * (0.05236) \quad [7.6]$$

$$\sigma_{effPm-147^g} = 7.596E-23cm^2 * \left(\frac{1b}{1E-24cm^2} \right) = 76b \text{ w/o burnup} \quad [7.7]$$

From Equation 6.3 above, the effective cross section of Pm-147 to Pm-148g calculated from the values for the thermal and epithermal cross sections found in literature is 138.5 barns. The following is a difference calculation:

$$\frac{138.5b - 76b}{138.5b} = 0.451 = 45.1\% error \quad [7.8]$$

Similarly,

$$\sigma_{effPm-147^m} = 3.91E-23cm^2 * \left(\frac{1b}{1E-24cm^2} \right) = 39.1b \text{ w/o burnup} \quad [7.9]$$

From Equation 6.3 above, the effective cross section of Pm-147 to Pm-148m calculated from the values for the thermal and epithermal cross sections found in literature is 98.7 barns and thus produces a difference of 60.4%. Thus, calculating the cross section without considering burnup of Pm-148 ground and metastable states does not provide a very accurate calculation.

7.3 Promethium-147 Cross Section Calculation with Burnup

In order to have a more realistic result for cross section of Pm-147, one must take into account the burnup of Pm-148. The following equations are used:

$$\frac{dN_{148g}}{dt} = N_{Pm-147}\sigma_{effPm-147}\phi - (\lambda_{Pm-148g} + \phi\sigma_{Pm-148g})N_{Pm-148g}$$

$$\frac{dN_{148g}}{dt} = \Lambda_{Pm-147}N_{Pm-147} - \Lambda_{Pm-148g}N_{Pm-148g}$$

$$A_{148g} = \lambda_{148g}N_{Pm-148g} = \lambda_{148g}N^0_{Pm-147} * \frac{\Lambda_{Pm-147}}{\Lambda_{Pm-148g} - \Lambda_{Pm-147}} \left(e^{-\Lambda_{Pm-147}t} - e^{-\Lambda_{Pm-148g}t} \right)$$

Where:

$$\Lambda_{Pm-147} = \sigma_{effPm-147}\phi$$

$$\Lambda_{Pm-148g} = \lambda_{Pm-148g} + \phi\sigma_{Pm-148g}$$

Substituting values and solving for Λ_{Pm-147^g}:

$$3.0525E-8 = \Lambda_{Pm-147^g} * \left[e^{-\Lambda_{Pm-147} * 3.6E4} - 0.81214\right]$$

This equation requires solving by iteration: $\Lambda_{Pm-147^g} = 1.68E-7cm^2$

$$\sigma_{effPm-147^g} = \frac{\Lambda_{Pm-147^g}}{\phi} = \frac{1.68E-7cm^2}{2.05E15} = 8.20E-23cm^2$$

Substituting values and solving for Λ_{Pm-147^m}:

$$6.375E-8 = \Lambda_{Pm-147^m} * \left[e^{-\Lambda_{Pm-147^m} * 3.6E4} - 0.412811\right]$$

This equation requires solving by iteration: $\Lambda_{Pm-147^m} = 1.093E-7cm^2$

$$\sigma_{effPm-147^m} = \frac{\Lambda_{Pm-147^m}}{\phi} = \frac{1.093E-7cm^2}{2.05E15} = 5.33E-23cm^2$$

7.4 Promethium-148m and Promethium-148g Cross Section Calculation

The cross section of Promethium-148m and Promethium-148g can be calculated using Isochain. Isochain is used because the thermal and epithermal cross sections can be changed, and the resulting estimate of Promethium-148 production can be compared to the amount of Promethium-148 metastable and ground state produced in the reactor at end of bombardment. The end of bombardment activity is calculated by using CLSQ, as shown in Figure 7.2-7.4 above. The thermal and epithermal cross sections are modified until the production estimate at end of bombardment (in this case 10 hours) is approximately equal to the activity at the end of bombardment that was calculated using CLSQ. Table 7.3 contains the values for Pm-148m and Pm148g cross sections and Figure 7.5 shows the activity at end of bombardment compared to the estimated Isochain production curves before cross section manipulation.

Table 7.3: Known Cross Section Values of Promethium-148g and Pm-148m[12]

[b]	Pm-148m	Pm-148g
σ	10600±1000	2000±1000
I	3600±2400	679.2

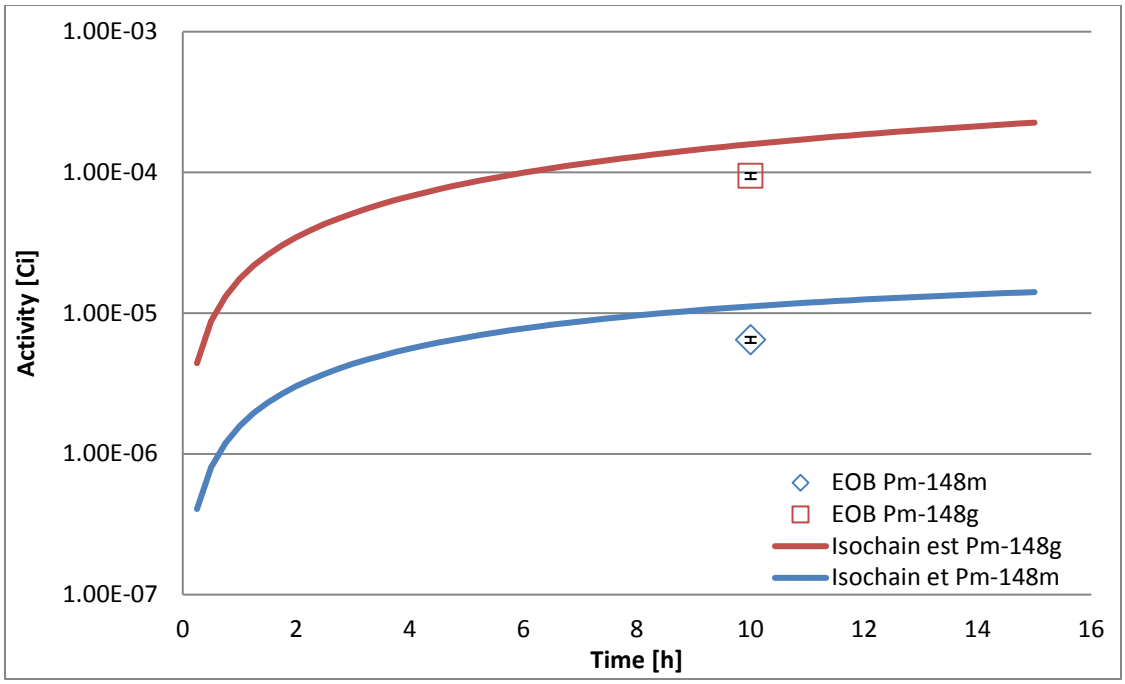

Figure 7.5: End of Bombardment Points and Isochain Estimate using Known Values

The epithermal cross section of Pm-148g is listed in Reference 12 as "0" but we understand that this is not accurate. Instead, it is assumed that it has the same relationship to the Pm-148g thermal cross section:

$$\frac{3600b}{10600b} = \frac{I}{2000b}$$

$$I = 679.2b$$

To begin, the Pm-148 metastable thermal cross section was increased to 31000 b and the epithermal cross section was increased by the same ratio, to 10528b.

$$\frac{3600b}{10600b} = \frac{I_{new}}{3600b}$$

$$I_{new} = 10528b$$

This assumes that the ratio of thermal cross section to epithermal cross section remains constant. Isochain was executed with the new cross sections for Pm-148m. Manipulations of the cross sections, being careful to change the epithermal cross section by the same ratio every time, were made and then Isochain executed again until the Isochain estimate was approximately equal to the amount actually produced. This determined that the thermal cross section of Pm-148m is 29900b and the epithermal cross section of Pm-148m is 10155. Once the cross sections for Pm-148m were found, they were held constant and the process was repeated in order to find the

thermal and epithermal cross sections of Pm-148g. Table 7.4 contains the reported cross sections and the cross sections that were calculated in this project. Figure 7.6 contains the End of Bombardment result from CLSQ with the Isochain estimate produced by manipulating the cross section.

Table 7.4: Isochain-Calculated Cross Sections

	Reported		Calculated	
[b]	Pm-148m	Pm-148g	Pm-148m	Pm-148g
σ	10600±1000	2000±1000	29900±1495	17970±899
I	3600±2400	679.2	10155±508	6103±305

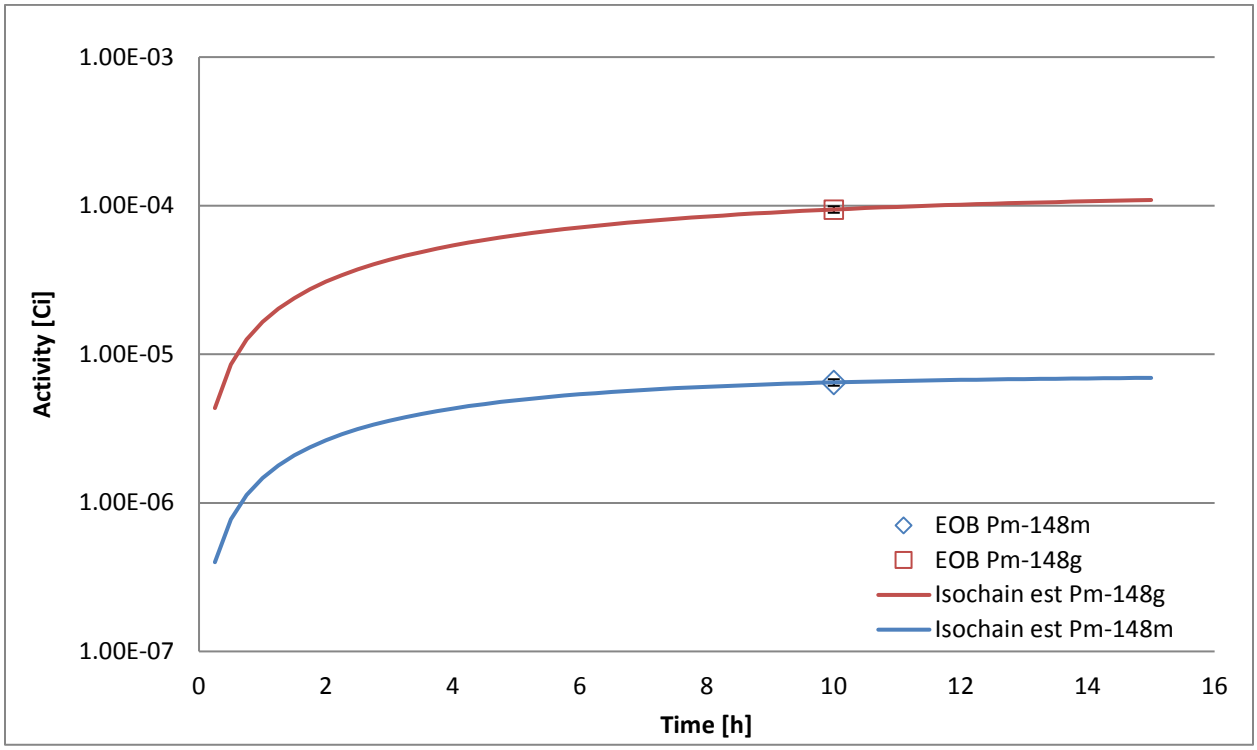

Figure 7.6: Isochain-Calculated Cross Sections

In order to calculate error, one must realize that the cross section error is equal to the relative error from CLSQ for EOB activity. For Pm-148m, the result from CLSQ is 2.02E2±3.291E-1 counts per minute. The Relative Error of the EOB activity as calculated by CLSQ for Pm-147 is:

$$\frac{\sigma}{x} = \frac{3.291E-1cpm}{2.02E2cpm} = 1.629E-3$$

Assuming that the error on the detector efficiency is 5% and adding these two in quadrature, the fractional error of the activity of Pm-148m is:

$$\sqrt{(1.629E-3)^2+(0.05)} \approx 0.05$$

The absolute error of the activity of Pm-148m in the entire sample is then:

$$Error * Activity = 0.05 * 6.4648E-6Ci = 0.323E-6Ci$$

Therefore, the activity of Pm-148m in the entire sample is 6.465E-6±0.323E-6 curies. The absolute error of the cross sections of Pm-148m is:

$$Error * (\sigma_t) = 0.05 * 29900b = 1495b$$

$$Error * (I) = 0.05 * 10155b = 507.78b$$

Therefore, the thermal cross section and resonance cross section of Pm-148m is 29900±1495b and 10155±508b, respectively. The error calculation for cross sections of Pm-148g is the same and Table 7.5 below contains all of the cross sections.

Table 7.5: Thermal and Resonance Cross Sections of Pm-148m and Pm-148g

8. Conclusions and Future Work

This research successfully verified the predictions and accuracy of the computer codes CLSQ and Isochain. These two programs will be able to be used in future research on the production of Pm-147 in hopes of producing large quantities. The analysis showed that there was very little difference in the result of both programs for the amount of decay time needed to have use of the Pm-147. The Nd-147 must be allowed to decay for 153 days in order for the characteristic 121 keV gamma ray from the Pm-147 to be seen and utilized in applications.

Analysis utilizing the Oak Ridge National Laboratory's High Flux Isotope Reactor allowed for absorption effective cross section determination of Pm-147. The cross section for neutron bombardment of Pm-147 to form Pm-148 ground state is 76 barns, and the cross section for neutron bombardment of Pm-147 to form Pm-148 metastable state is 39.1 barn without burnup considerations.

Future work will be required in order to scale the production experiment to quantities useful in nuclear battery applications. CLSQ and Isochain will be central to future analysis of Pm-147.

LIST OF REFERENCES

[1] Oak Ridge National Lab (ORNL) Nuclear Medicine Group (NMG) procedure NMG-49 - *Procedure for the Loading, Testing, Certification, and Irradiation of HFIR Hydraulic Tube Capsules*

[2] ORNL Nuclear Medicine Group (NMG) procedure NMG-52 - *HFIR Irradiation Unit - Helium Leak Test*

[3] "ORNL Nuclear Medicine Program Develops Efficient Method for Separation of Promethium-147 from Reactor-Produced Neodymium-147" Isotope News, Vol. 1, Issue 1, pg 5-7

[4] Atlas of Neutron Resonances 5th Edition (BNL-325), S. F. Mughabghab 2006

[5] Chart of the Nuclides 16th Edition, Lockheed Martin 2002

[6] Akhil, P., "Nuclear Battery," MES College of Engineering, 2008.

[7] Ragheb, M., "Radioisotopes Power Production" February 15, 2011

[8] E. Browne, R.B. Firestone, V. Shirley, "Table of Radioactictive Isotopes," Lawrence Berkely National Lab, 1986

[9] M.A. Garland, S. Mirzadeh, C.W. Alexander, G.J. Hirtz, R.W. Hobbs, G.A. Pertmer, F.F. Knapp Jr., "Neutron Flux Characterization of a Peripheral Target Position in the High Flux Isotope Reactor," Applied Radiation and Isotopes, Vol. 59, pgs. 63-72.

[10] Isotopic and Spectrographic Analysis for Neodymium Batch# 161701, ORNL

[11] ENDF Nuclear Wallet Cards: http://www.nndc.bnl.gov/nudat2/indx_sigma.jsp

[12] S.F. Mughabghab, "Atlas of Neutron Resonances: Resonance Parameters and Thermal Cross Sections," NNDC and Brookhaven National Laboratory, El Sevier Publishing, 5th Edition, 2006

[13] "The High Flux Isotope Reactor at ORNL," http://neutrons.ornl.gov/facilities/HFIR/

[14] "Isochain Introduction," Oak Ridge National Laboratory, June 25, 2010

[15] R.B. Firestone, V. Shirley, "Table of Isotopes CD ROM Edition," Wiley-Interscience, Version 1.0, March 1996

[16] C.M. Lederer, V. Shirley, "Table of Isotopes," Wiley-Interscience, Seventh Edition, 1978

[17] J.B. Cumming, "CLSQ, The Brookhaven Decay Curve Analysis Program", National Academy of Sciences Report # NAS_NS 3107, p25-33, 1962

[18] “Least Squares Fitting,” http://mathworld.wolfram.com/LeastSquaresFitting.html

[19] “Web Elements,” www.webelements.com

[20] A.H. Wapstra and N.B. Grove, “Part I. Atomic Mass Table”

[21] J.H. Hinderer, “Radioisotopic Impurities in Promethium-147 Produced at the ORNL High Flux Isotope Reactor (HFIR),” UT Knoxville, May 2010